From the Department of Neuroscience, Karolinska Institutet,
and the Department of Sport and Health Sciences,
Idrottshögskolan, Stockholm, Sweden

BIOMECHANICS OF BACK EXTENSION TORQUE PRODUCTION ABOUT THE LUMBAR SPINE

Karl Daggfeldt

Stockholm 2002

Published and printed by Karolinska University Press
Box 200, SE-171 77 Stockholm, Sweden

ISBN 91-7349-107-1

"It does not do harm to the mystery to know a little bit about it.”

Richard Feynman

ABSTRACT

The aim of this thesis has been to develop a realistic mechanical description of lumbar back extension torque production. Such a description is desirable for understanding how back extension torque is generated as well as how the spine and surrounding structures are loaded during back extension tasks.

Investigations utilising anatomical images from the Visible Human Project revealed that many of the erector spinae fascicles originating from the lumbar levels attached to the erector spinae aponeurosis covering the dorsal part of the muscles. This observation was contradicting the descriptions used in previous detailed back extension models. The different interpretation of the muscle geometry will have implications for the modelling of both lumbar torque production and lumbar spinal loading. The Visible Human data were also used to map the detailed anatomy of the multifidus and quadratus lumborum. Except for the thoracic part of multifidus, which has not been investigated in detail before, these muscles did not show any major deviations from earlier studies.

A model of the mechanisms involved in intra-abdominal pressure (IAP) induced unloading of the lumbar spine was generated in order to clarify some controversies from the literature. It was shown that the unloading mechanism could be viewed as a pressurised column, with the maximally possible cross-sectional area restricted in size by the smallest abdominal transverse cross-sectional area, pushing the rib cage and pelvis apart. An abdominal form with zero longitudinal curvature was found to have some important mechanical benefits for the generation of IAP induced alleviation of compressive loading of the lumbar spine. In combination with physiological measurements of back extensor torque, IAP and abdominal geometry, the model-calculation showed a possibility for contributions from IAP to lumbar extensor torque production of about 10% of the total maximal voluntary back extensor torque, and reductions of spinal compression of up to 40% as compared to torque creation without IAP.

Magnetic resonance imaging was used to study the effect of mechanical changes due to varying flexion-extension in the lumbar spine. It was observed that the back extensor muscles tended to increase their lever arm lengths when the spine was extended. This would imply less need for muscle force in order to create a given torque in the extended as compared to the flexed position. Contrary to this the spinal unloading effect from the IAP was greatest with the spine held in a flexed position. Since these two opposing effects were of the same magnitude it is not evident which posture will reduce mechanical loading for a given torque production.

The model was tested in different ways. By generating IAP through stimulation of the phrenic nerve it was shown that IAP could generate extensor torque about the lumbar spine reasonably well according to model predictions. The specific muscle tensions needed to generate measured maximal voluntary back extension torques agreed well with *in vitro* measurements of maximal tension from the literature. The model could generate close to simultaneous equilibrium about all the lumbar discs simply by a uniform muscle activation of all back extensor muscles.

Key words: Biomechanics, model, back extension, Visible Human, intra-abdominal pressure, lever arm, erector spinae, back extension

LIST OF PUBLICATIONS

I Tveit, P., Daggfeldt, K., Hetland, S., Thorstensson, A. Erector Spinae Lever Arm Length Variations with Changes in Spinal Curvature. Spine, 1994, 19, 199-204

II Daggfeldt, K., Thorstensson, A. The role of intra-abdominal pressure in spinal unloading. Journal of Biomechanics, 1997, 30, 1149-1155

III Daggfeldt, K., Huang, Q.-M., Thorstensson, A. The Visible Human Anatomy of the Lumbar Erector Spinae. Spine, 2000, 25, 2719-2725

IV Hodges, P.W., Cresswell, A.G., Daggfeldt, K., Thorstensson, A. In vivo measurement of the effect of intra-abdominal pressure on the human spine. Journal of Biomechanics, 2001, 34, 347-353

V Daggfeldt, K., Thorstensson, A. The mechanics of back extensor torque production about the lumbar spine. Journal of Biomechanics, 2001, submitted

CONTENTS

LIST OF ABBREVIATIONS

ACSA	Anatomical cross-sectional area
e	Unit vector
e.g.	For example
EMG	Electromyography
ES	Erector spinae
ESA	Erector spinae aponeurosis
et al.	And others
F	Force vector
i.e.	That is
IAP	Intra-abdominal pressure
L#	Lumbar vertebra number
LIA	Lumbar intermuscular aponeurosis
Lim	Limit
m	Mass
MR	Magnetic resonance
PCSA	Physiological cross-sectional area
r	Position vector
S#	Sacral vertebra number
t	Time
T#	Thoracic vertebra number
v	Velocity vector
VH	Visible Human

1 BACKGROUND

1.1 INTRODUCTION

The objective of this thesis has been to develop a realistic mechanical description of lumbar back extension torque production. Such a model is desirable for understanding how back extension torque is generated as well as how the spine and surrounding structures are loaded during back extension tasks. Before getting into the particulars let us first take a step back to get a feeling for the connections to science at large.

The founding principle of science is that truth only can be judged from observation of reality. During the scientific revolution some influential individuals questioned the uncritical acceptance of words from authorities like Aristotle and the Bible. They chose to trust models of reality only as far as they agreed with experimental observation. This attitude was expressed by the motto of the Royal Society "Nullius In Verba" (nothing from words). From this idea the explosive development of science, that we still are part of, emerged. As the amount of scientific information has grown, the scientific community has partitioned into subgroups spanning different parts of natural phenomena with scopes ultimately limited by the capacity of the human brain to incorporate and process information. The subject of this thesis is contained in the field of Biomechanics, which derives from the Greek βίος (life) and μηχανή (machine). It refers to the science of mechanics applied to living organisms. The word is not old, it was possibly coined 1887 by the Austrian professor Moriz Benedikt (Benedikt, 1910), but relevant issues have been addressed at least since 1638 when Galileo Galilei discussed the scaling of animal bones (Galilei, 1954). There are no special fundamental laws for living matter, only the laws of physics. The complexity of biological systems, however, makes it impossible to reduce all information of interest for our understanding of living mechanical systems to the laws of physics. Biomechanics therefore merits as a separate research field, interdisciplinary between mechanics and biology.

It has been my aim to give the layman, at least to some degree, a chance to understand the scientific foundation for the thesis, based on experimental observations. This was considered feasible for classical mechanics, since it can be reduced to a few fundamental laws. Section 1.2 serves that purpose as well as introducing the mathematical tools and language used in the thesis. Readers familiar with classical mechanics and basic calculus could go directly to section 1.3 without loosing any information specifically related to the thesis objectives. For the biological side the experimental foundation rests too much on un-amalgamated high-level information to be succinctly presentable. Thus, it must, to a large extent, be referred to via references.

1.2 FUNDAMENTAL MECHANICAL LAWS AND MATHEMATICAL TOOLS

1.2.1 Limits

The mathematics of calculus is an important tool in mechanical reasoning. The unifying concept of calculus is to make use of a specially defined value, namely the value approached arbitrarily close by a function evaluated close enough to a given point (or infinity). Or, expressed differently, the limit of the function in the selected point (the formal definition can be found in any calculus textbook (e.g. Aleksandrov et al., 1999)). The limit can exist even though the function itself is not defined in the point. Two of Zeno's famous paradoxes, as stated in Aristotle's Physics (Aristotle, 1984), will be used to show some of the conceptual problems solved by our understanding of the rather subtle notion of limits. The first paradox, the Arrow,

deals with the problem of defining instantaneous velocity; "*everything when it occupies an equal space is at rest, and if that which is in locomotion is always in a now, the flying arrow is therefore motionless."* So, since at a point in time everything is in a fixed unmoved position, this seems to imply that nothing can move (if a time interval can be seen as a sum of time points). Since the development of calculus, brought to maturation by Newton and Leibniz (Boyer, 1949), we know that instantaneous velocity has to be defined as the value approached by the fraction of distance passed over a given time interval as the time interval approaches zero. Or, in other words, as the limit of distance over time as the time approaches zero. This definition can be generalised to describe the instantaneous rate of change of all continuous functions and it is called the function's derivative. Due to Leibniz we symbolise the derivative of a function f with respect to the variable x as df/dx. A finite change of a variable f is normally symbolised with the Greek Δ while the Latin d is used to indicate a change, in a limit, approaching zero. The full definition in mathematical symbolism is presented in equation (1.1).

$$\frac{df}{dx} = \lim_{\Delta x \to 0} \frac{f(x+\Delta x) - f(x)}{\Delta x} \tag{1.1}$$

The second paradox, the Dichotomy, deals with infinite sums; "*it asserts the non-existence of motion on the ground that that which is in locomotion must arrive at the half-way stage before it arrives at the goal."* So, moving even the slightest distance would imply first moving half that distance, then half the half distance and so on. Again it seems as nothing can move, unless an infinite number of distances can be traversed in a finite time. The resolution is that a finite amount of time or a finite length both can be divided into an infinite number of pieces. Such sums can be calculated as the limit of the sums as the number of terms approaches infinity. A limit like this is necessary for calculating the distance moved from a variable velocity function. The product of the velocity at one time with a time interval will not give the precise displacement (since the velocity is varying) but the errors will approach zero as the time interval approaches zero. The distance is then given as the limit of a sum of distances with the number of terms approaching infinity (so the time intervals approach zero). The generalisation of this concept gives the definition of integration. Already Archimedes utilised the principles of integration when he calculated the area of a segment of a parabola but the generalised definition is due to Newton and Leibniz (Boyer, 1949). The right side of equation (1.2) gives the full definition of the integral of a function f over a variable interval from x_0 to x_n and the left side gives the shorthand, again according to Leibniz.

$$\int_{x_0}^{x_n} f(x) \cdot dx = \lim_{n \to \infty} \sum_{i=1}^{n} (f(x_i) \cdot \Delta x) \tag{1.2}$$

One important limit that will be used subsequently is given by equation (1.3). The straightforward way to calculate a limit of a function like this would be to substitute its transcendental factors (here sinus) with their Taylor series. For readers unacquainted with this technique (derived in any calculus textbook, e.g. Aleksandrov et al., 1999), a well known geometrical proof of the limit is presented in figure 1.1.

$$\lim_{x \to 0} \frac{\sin x}{x} = 1 \tag{1.3}$$

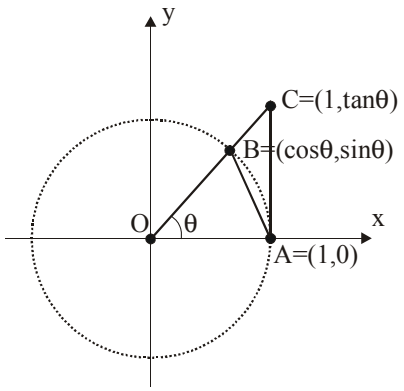

Figure 1.1. A standard geometrical proof of equation (1.3). Although it can be shown by integration we will grant the knowledge that the area of the unit circle sector OAB is θ/2 (or θ/2π of the total unit circle area π), where θ is measured as the ratio of the circle sector arc length by its radius (or in other words, it is measured in radians). It can be seen in the figure that this area is larger than the area of the triangle OAB but smaller than the area of the triangle OAC. This leads to the inequality; $\sin\theta/2 < \theta/2 < \tan\theta/2$. By the substitution $\tan\theta = \sin\theta/\cos\theta$ and some reshufflings, we obtain; $1 > \sin\theta/\theta > \cos\theta$. In the limit when θ approaches zero $\cos\theta$ will approach one (since $\cos 0 = 1$). Our function $\sin\theta/\theta$ is then, in the limit, squeezed between one and something that approaches one. So its limit must also be one.

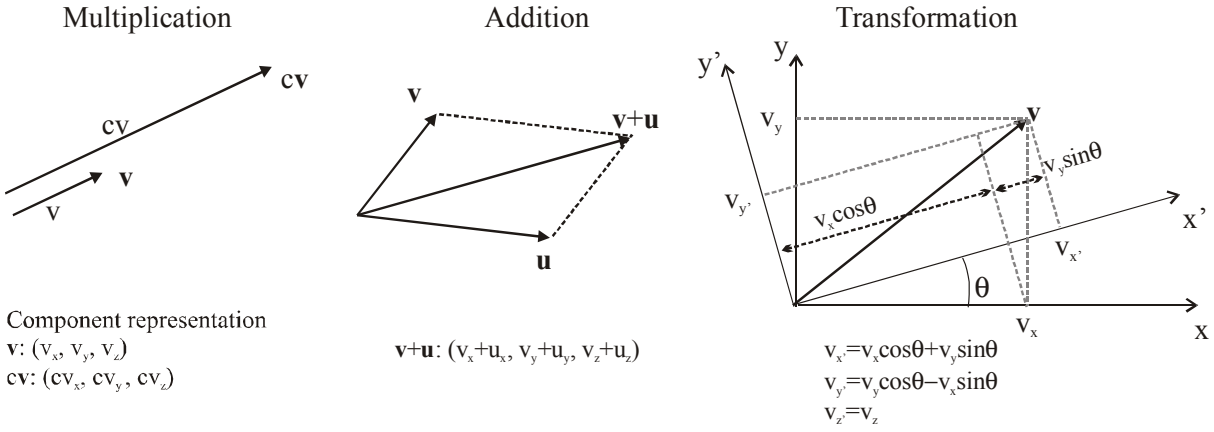

Figure 1.2. Graphical and component representations of multiplication with a number or a scalar (c), addition of two vectors (**v** and **u**) and transformation to a new coordinate system turned an angle θ about the z- axis. Multiplication with the number c makes the vector c times as long but does not change its direction (unless c is negative in which case the vector takes the diametrically opposed direction). Adding **v** and **u** will result in a vector **v**+**u** which can be constructed graphically as the arrow running from start to end of **v** and **u** placed head to tail (it can be seen in the parallelogram that both alternatives of putting **v** before **u** or the opposite will give the same result, so vector addition is commutative). The rules of vector addition are intuitively obvious when considering displacements, it just states that when making two consecutive displacements the resulting displacement will be the one carrying from the start to the end. The transformation rules can be figured out from trigonometrical considerations in the figure.

1.2.2 Vectors

Two different types of physical quantities are used in basic mechanics, scalars that are defined completely by their magnitude (like time and mass) and vectors that are defined completely by magnitude and direction (like displacement, velocity, acceleration and force). Any vector can be

represented by a displacement in space (often symbolised by an arrow) and must therefore add and multiply with constants like displacements. Like displacements each vector can also be specified by three components in a given coordinate system and its components must transform between different coordinate systems like those of displacements (figure 1.2). In this thesis summary vectors are represented symbolically with boldface (e.g. **v**) while the letter symbol without boldface (i.e. v) represents the size of the vector.

A vector can be defined as any entity whose components transform like displacements. It can easily be seen from the transformation laws in figure 1.2 that the product of a number (or a scalar) and a vector transforms between different coordinate systems like a vector. From this follows that velocity constitutes a vector (since, in the limit as Δt tend to zero, velocity can be expressed as the product of the scalar $1/\Delta t$ times the displacement $\Delta\mathbf{r}$). Similarly it can be shown that acceleration constitutes a vector. Experimental observations by men like the Dutch renaissance scientist Stevin have shown that forces also behave like vectors (Dugas, 1988).

There are two ways to combine the components of two vectors in order for the result to be unchanged after transformation to another coordinate system. These entities are of importance since they can represent real physical entities, which have to be invariant to coordinate transformations. First one can make a scalar of two vectors according to equation (1.4). This is referred to as scalar product. Geometrically it represents the length of the projection of either of the two vectors on to the direction of the other multiplied by the length of the latter. It will be used in the thesis to express the size of the projection of a given vector in a given direction (by creating the scalar product of the given vector by a vector of unit size in the given direction).

$$\mathbf{v} \cdot \mathbf{u} = v_x u_x + v_y u_y + v_z u_z \tag{1.4}$$

Secondly one can make a new vector (strictly speaking this constitutes a pseudo vector that differs from the true displacement type vectors by transforming differently when changing the handedness of the coordinate system) of the component products according to equation (1.5). This construction is called the vector product of **v** and **u** and it is symbolised $\mathbf{v} \times \mathbf{u}$. It can be seen from the definition that the vector product is not commutative.

$$\begin{aligned} (v \times u)_x &= v_y u_z - v_z u_y \\ (v \times u)_y &= v_z u_x - v_x u_z \\ (v \times u)_z &= v_x u_y - v_y u_x \end{aligned} \tag{1.5}$$

The geometrical interpretation states that the vector product $\mathbf{v} \times \mathbf{u}$ has the size of the area of the parallelogram with sides **v** and **u**, and is directed perpendicular to this parallelogram in such a way that turning a right hand screw from **v** to **u** (choosing the direction of the closest angle) would advance the screw along the direction of the vector. The vector product is often used for representing some type of "rotation quantity" (like angular velocity or torque), where the vector is directed along the axes of rotation and the rotation represented is directed as the rotation of the right hand screw.

The vector analysis as we know it today was first developed by Gibbs (Gibbs and Wilson, 1960). Some of the mechanical laws are most conveniently expressed as vector equations (e.g. equation (1.6)). One such equation represents the equality of the components of the two sides of the equation as resolved in any applicable coordinate system. So, except for saving space by expressing three equations in one, a vector equation also has the advantage of staying free from

any specific coordinate system. The fact that the laws of physics can be expressed as vector equations stems from the experimental observation that a self-contained physical system will act the same independently of its orientation in space (rotational invariance).

1.2.3 Newton's laws of motion

Classical mechanics was given a solid foundation by Newton's three laws of motion (Newton, 1999). The first law states that an object will move with constant velocity along a straight line unless it is acted on by force. This can seem contrary to intuition. Due to friction objects in our environment tend to slow down. The wagon stops when the horses stop pulling. A thrown object soon comes to a halt on the ground. Observations like this make it easy to believe that objects will be at rest without the influence of force. Aristotle was of this belief (Aristotle, 1984). He even constructed a far-fetched explanation for how a projectile can keep a forward motion in the air, based on the formation of a pushing airflow around the projectile. After the new Copernican worldview, where the earth is moving around the sun, it, however, became clear that rest is a relative concept. What appears to be at rest here moves with great speed if viewed from another celestial body, or just from the other side of the spinning earth. Galileo realised that a new understanding of motion and force was needed. He drew some important conclusions from experiments (Galilei, 1954) which paved the way for Newton. Indirectly, by observing the nature of a pendulum, he assumed that a ball rolling down an inclined plane would roll up a second plane, of arbitrary inclination, to the same height as it was dropped from, provided the work of friction could be abolished (figure 1.3). In such case, the ball would continue in perpetual motion if the inclination of the second plane were reduced to zero. It was experiments and deductions like these that made Galileo understand that motion undisturbed by forces will continue with constant speed, the basis of Newton's first law (although Newton had to straighten the circular motion which Galileo assumed to be the natural path). Strictly speaking the first law is superfluous, since it constitutes a special case of the second law, but it serves as a helpful first mental preparation for understanding the second law.

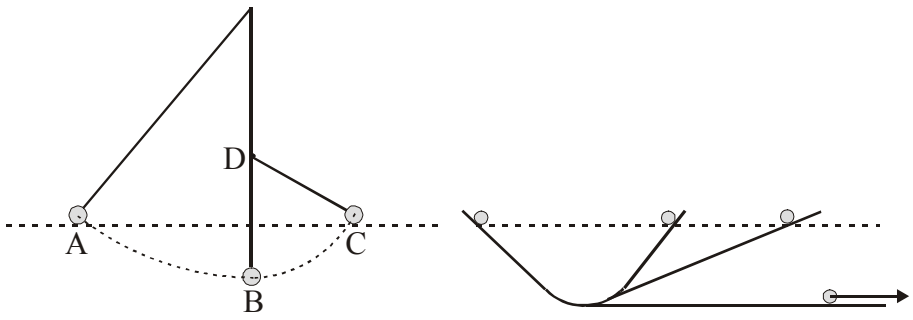

Figure 1.3. To the left, a pendulum that, after moving from A to B, gets a new centre of rotation when the line is hitting a bar at D. The same height is reached in A and C. This led Galileo to the assumption that balls rolling down and up inclined planes, as shown to the right, also would reach the same height, provided the work of friction could be abolished. The ball must then keep perpetual motion if the inclination of the second plane is reduced to zero.

Newton's second law of motion describes the interplay between force and motion (Newton, 1999). With modern vocabulary it says that the force (**F**) on a mass particle (a piece of matter in a limit approaching zero extension in space) equals its mass (m) times the time-derivative of its velocity (**v**), where both force and velocity constitute vectors (equation (1.6)). By integration it

can be shown that the same equation holds for a body of constant mass with finite extension in space, the velocity then becoming the velocity of the body's centre of mass (the arithmetic mean of the mass particles' masses times their positions in space).

$$\mathbf{F} = m \cdot \frac{d\mathbf{v}}{dt} \tag{1.6}$$

Also for the second law it was Galileo who made the first crucial conclusions from experimental observations (Galilei, 1954). Once again small balls rolling along inclined planes contributed to reveal the secrets of nature. By weighing the amount of water flowing out of a small hole in a bucket during a given ball movement Galileo could deduce the time course of the descent. He noted that the weight of the ball did not influence the speed. Perhaps less dramatic than dropping weights from the leaning tower of Pisa (an experiment of which Galileo left no record) the rolling balls on inclined planes constituted a much more suitable experimental setup, since the effects of air resistance (which would effect the conclusion) could be made negligible with the slower motion. He also noted the relation between the inclination of the plane and the time of descent. It was, however, up to Newton to formulate the general relation between movement and force. He understood that the component of the gravitational force along the inclined plane was proportional to the acceleration. Since the gravitational force is proportional to mass, whereas the acceleration is independent of mass, he also could conclude that acceleration must be inversely dependent on mass. The second law for one dimension was thus to a large degree deduced from Galileo's observations. Newton got the idea, when watching an apple fall, that all bodies are attracted to each other due to their masses (Newton, 1999). What makes the apple fall is the mutual attraction between the apple and the earth. Maybe, he thought, it is the same gravitational force that keeps the planets moving around the sun. The vector character of the second law was then confirmed in the most magnificent way, by showing that Kepler's laws describing the planetary motions automatically would follow from the second law, provided that a gravitational force was acting between the planets and the sun, with a magnitude inversely proportional to the square distance to the sun (so at the same time the gravitational law was formulated).

Newton's third law of motion states that any forces acting between two bodies always are equal in size and opposite in direction (Newton, 1999). Wallis, Wren and Huygens, three contemporaries of Newton, all contributed to show that the total momentum (a vector quantity given by mass times velocity) is constant before and after impacts between bodies (Dugas, 1988). From this it can be deduced that the bodies during the impact must influence each other with impulses (forces integrated over time) of equal size and opposite direction (figure 1.4). This was one of the leads for formulating the third law.

Newton also argued for the third law from everyday experience (Newton, 1999). If, for example, two different parts of a solid body would influence each other with unbalanced forces then the object would accelerate in the direction of the resulting force, according to the second law, without external influences. This is not what can be observed in reality. We do not expect objects at rest to start moving unless acted on by some external force. The third law implies that the sum of all internal forces in a body will cancel each other out so that only the external forces will contribute to the average motion (e.g. the motion of the centre of mass) of the body. What was not explicitly stated in the third law was that the forces between two bodies also must act along the same line. Otherwise could, for instance, a solid object at rest start rotating without any external influence. In figure 1.5 the complete laws of motion have been expressed in a concise form. It is the charm of classical mechanics that, together with some information about

how forces are generated, these laws of motion can explain a vast amount of different phenomena, from the motion of the celestial bodies to the mechanics of back extension.

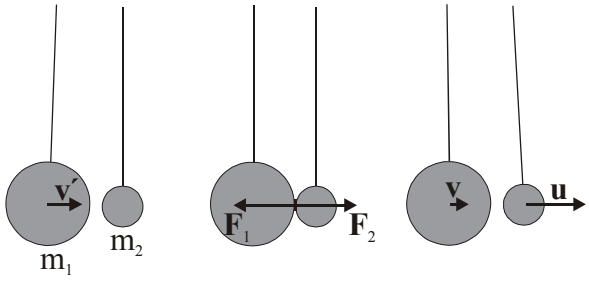

Figure 1.4. Observations on, for instance, pendulums showed that momentum is conserved during impacts between bodies, leading to the conclusion that they must influence each other with impulses of equal size and opposite direction. Here the left pendulum with mass m_1 is moving with speed $\mathbf{v}'$ while the right pendulum is at rest just before the impact. After the impact the left and the right pendulums have the speeds $\mathbf{v}$ and $\mathbf{u}$ respectively. Conservation of momentum infers; $m_1\mathbf{v}' = m_1\mathbf{v} + m_2\mathbf{u} \Rightarrow m_1\Delta\mathbf{v} = -m_2\Delta\mathbf{u}$. By integrating equation (1.6) to get the impulse $\int \mathbf{F}dt = m\Delta\mathbf{v}$ and comparing with the previous equation it shows that the impulses on the two pendulums must be of equal size and in opposite direction. By observation of the constancy of momentum also during the impact one could conclude $\mathbf{F}_1 = -\mathbf{F}_2$.

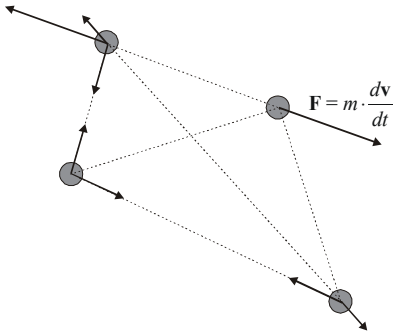

Figure 1.5. Four mass particles (for visibility drawn finitely) interacting according to the laws of motion, which concisely can be stated as follows. All forces are created through interaction between mass particles. Between two particles this interaction constitutes forces of equal size and opposite direction acting along the line connecting the particles. The resulting force on a given mass particle will affect its motion according to Newton's second law of motion (equation (1.6)).

1.2.4 The torque equation

A useful theorem (equation (1.7)) can be derived by vector multiplying a displacement vector $\mathbf{r}$ from any given fix point to a mass particle on both sides of equation (1.6). By applying the product rule of derivation, as deduced in most calculus textbooks (e.g. Aleksandrov et al., 1999), to the right hand side of equation (1.7) and observing that the vector product of two parallel vectors equals zero one can show that it equals the vector product of $\mathbf{r}$ times the right hand side of equation (1.6). The equation (1.7) states that the torque ($\mathbf{r}\times\mathbf{F}$) acting on the particle equals the time derivative of its angular momentum ($\mathbf{r}\times m\mathbf{v}$).

$$\mathbf{r} \times \mathbf{F} = \frac{d(\mathbf{r} \times m\mathbf{v})}{dt} \tag{1.7}$$

It follows from equation (1.7) that the sum of all torques (since torques from internal forces always will cancel each other out, only torques from external forces will have to be considered) acting on the mass particles' in a body (about a given fix point) will equal the time derivative of the particles summed angular momentum (calculated about the same fix point). In a static situation where the angular momentum does not change, equation (1.7) states that the total torque about any fix point has to vanish. Perhaps this can be understood more intuitively by noticing that in a static situation where no mass particle in a body has any acceleration each particle must be in force equilibrium. External and internal forces on each particle must therefore be of equal size and opposite direction. The external forces could therefore be obtained simply by changing the direction of all the internal forces to the diametrically opposite direction. Since the size of the torque will remain the same after such an operation (it only changes to the opposite direction) and the sum of the torques from the internal forces, since they appear in pairs with cancelling torques, always vanish (independently of any equilibrium demands) the sum of the torques from the external forces must, in this case, also vanish.

The size of a torque created by a force about a given fix point can be expressed as the product of the force size and the length of something called the force lever arm. It can be understood from the definition of the vector product how the lever arm must be defined. As stated in section 1.2.2, the size of the vector product equals the area of the parallelogram spanned by the constituting vectors. The area of a parallelogram equals its base times its height, so if the force is chosen as the base in the parallelogram spanned by **r** and **F** the size of the torque can be expressed as the size of the force times the height of the parallelogram. This height must then equal the force lever arm length. It can be measured as the shortest distance from the fix point to a line, parallel to the force, drawn from the point of force application. The size of the angular momentum can be expressed similarly as the product of the momentum size and the length of the momentum lever arm.

1.3 BIOMECHANICAL MODELS OF BACK EXTENSION

In order to formulate the equations governing the interplay between forces and motion of a given body it is necessary to establish all the forces acting on the body through interaction with matter outside the body. Such forces are called external forces as opposed to internal forces that constitute interaction between different parts of matter inside the studied body. Newton's third law of motion implies that the sum of the internal forces is zero and the added prerequisite of force interactions along the same lines implies that the sum of all torques created by the internal forces also must be zero. Hence, only external forces can contribute to the total force and torque acting on the system. A good way to start defining the mathematical model is thus to draw the studied body with all its external forces. Such a drawing is called a free body diagram. The free body considered should preferably be chosen so that the forces of interest become external and so that other external forces become as few and easy to deal with as possible. When modelling loading of the disc between the fifth lumbar vertebra and sacrum (L5/S1 disc) Aspden (1989) chose to consider the spine as a free body. Unfortunately, an inappropriate mixing of the concepts of external and internal forces limits the conclusions from his study. It is otherwise perfectly feasible to use the spine (as with any other body) as the free body, although the great number of external forces acting on the spine (from, for example, muscles and tendons connecting to the spine) makes the problem rather complex. Instead, by choosing as the free

body the whole upper body divided by a transversal cut through a lumbar disc the number of external forces can be drastically reduced (Figure 1.6).

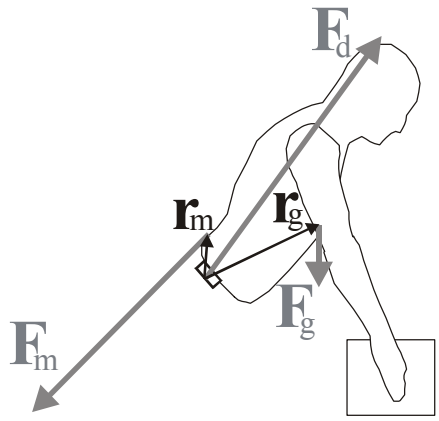

Figure 1.6. A free body diagram of the upper body, cut through the L5-S1 disc, in a lifting situation. The external forces are drawn with grey arrows ($\mathbf{F}_g$=gravitational force of upper body and lifted load, $\mathbf{F}_m$=muscle force, $\mathbf{F}_d$=load on the L5-S1 disk) and the displacements from the point of application of $\mathbf{F}_d$ to the forces' points of applications are drawn with black arrows ($\mathbf{r}_m$, $\mathbf{r}_g$).

The equations of movement for the free body in a static situation are then given by force and torque equilibrium (equations (1.8) and (1.9)). The point of application for the disc load has been chosen for the formulation of torque equilibrium. This is practical (although any point could have been used) since the disc load then will be excluded from equation (1.9). From an estimation of the gravitational force, its centre of gravity and the geometry of the back extensor muscles the size of the muscle force will follow from equation (1.9). Actually the problem of determining the muscle force is indeterminate since there are several different back extensor muscles that can contribute in different amounts (allowing an infinite numbers of different solutions). This problem is usually solved by some assumption, like for instance equal tension of all back extensors. Such assumptions can, to some degree, be tested by measurements like electromyographical recordings.

$$\mathbf{F}_g + \mathbf{F}_m + \mathbf{F}_d = 0 \tag{1.8}$$

$$\mathbf{r}_m \times \mathbf{F}_m + \mathbf{r}_g \times \mathbf{F}_g = 0 \tag{1.9}$$

It is seen from equation (1.8) that the disc is loaded by the sum of the gravitational force and the muscle force. From equation (1.9) and figure 1.6 it can be understood that the back extensor muscle force has to be much larger than the gravitational force since it has a shorter lever arm about the point of application of the disc load. The back extensor muscles passing this level therefore create the main part of the load on a given level of the lumbar spine. From this basic model one can understand that both a reduction of the lever arm length of the gravitational force and an increase of the lever arm length of the muscular force would reduce the need for muscle force and therefore also the load on the spine.

In the dynamic situation the derivative of the upper body momentum and angular momentum (this information would have to come from movement recordings) would have to be added as extra terms to the right side of equation (1.8) and (1.9) respectively (compare equations (1.6) and (1.7)). This type of basic biomechanical model for studying back extension tasks has been used at least since the study of Chaffin (1969). This thesis has aimed at creating a

more refined model, partly by generating better anatomical information about back extensor muscles and partly by studying the mechanics of intra-abdominal pressure (IAP). It will be shown that IAP can contribute an important external force that has been omitted in the free body diagram of figure 1.6 and in most previous models.

1.3.1 Back extensor muscle anatomy

The geometry of the lumbar back extensor muscles must constitute an integral part of any biomechanical back extension model. First back extensors were represented by a single muscle equivalent (e.g. Chaffin, 1969). More realistic models have since been developed (McGill and Norman, 1986; Macintosh et al., 1993; Bogduk et al., 1992; Stokes and Gardner-Morse, 1995). There has been some discussion in the literature concerning the anatomy of erector spinae, the main back extensor muscles, as used in these model studies.

The part of erector spinae that transmits force over the lumbar spine consists of iliocostalis lumborum and longissimus thoracis (Bogduk, 1980; Bustami, 1986; Winkler, 1937). These muscles are referred to as the lumbar erector spinae and can both be further divided into a thoracic and a lumbar part. The thoracic muscles have their rostral attachments at the thoracic level and the lumbar muscles at the lumbar level. The long caudal tendons of the thoracic fascicles contribute to the erector spinae aponeurosis (ESA), which covers erector spinae dorsally in the lumbar region and attaches caudally to the iliac crest and sacrum. Recent detailed anatomical studies show fair agreement in the description of the thoracic part of the lumbar erector spinae (Bogduk, 1980; Bustami, 1986). Ventral to the ESA and caudal to the thoracic fascicles inserting into it are the lumbar fascicles. Dissection studies of this part of the lumbar erector spinae show discrepancies both in nomenclature and gross morphology. Bustami (1986) refers to all the lumbar fascicles of the lumbar erector spinae as part of longissimus thoracis. He describes four laminae arising from the accessory processes and transverse (or costal) processes of the four uppermost lumbar vertebrae. The three superior laminae were observed to have caudal attachments to the iliac crest via the ESA while the most caudal lamina (from L4) was reported to have a direct muscular attachment to the iliac crest. Bogduk and Macintosh (Macintosh and Bogduk, 1987; Bogduk, 1980) found it more appropriate to divide the lumbar fascicles into a medial part belonging to longissimus thoracis and a lateral part belonging to iliocostalis lumborum. They reported rostral attachments of the longissimus thoracis part from the accessory processes as well as the medial three-quarters of the transverse processes of all lumbar vertebrae and rostral attachments of the iliocostalis lumborum part from the lateral quarter of the transverse processes as well as from the laterally adjacent thoracolumbar fascia. All caudal attachments were described as separated from the ESA. The four rostral fascicles (L1-L4) of the longissimus thoracis part were reported to attach caudally to the iliac crest via an aponeurosis inside the muscle mass, the lumbar intermuscular aponeurosis (LIA), while the L5 fascicle was found to have a direct muscular attachment to the iliac crest and associated sacroiliac ligament. All four lumbar fascicles of iliocostalis lumborum were reported to have direct attachments to the iliac crest.

Although the differences in muscle geometry due to these different anatomical descriptions can be considered as moderate it has been shown that even small variations can cause considerable alterations in model-predicted muscle and spinal forces (Nussbaum et al., 1995). It is therefore of importance to resolve the above mentioned controversy.

Furthermore, most detailed models of back extensor muscles (Macintosh et al., 1993; Bogduk et al., 1992; Stokes and Gardner-Morse, 1995) have not incorporated the quadratus lumborum muscle although this muscle has a mechanical leverage to create back extension

torque about the lumbar spine (e.g. Dumas et al., 1991) and has been shown to be co-activated with erector spinae in back extension tasks (Andersson et al., 1996).

With the Visible Human Project from the US National Library of Medicine a new powerful basis for anatomical investigation has become available. The project provides densely spaced transverse digital images from a male and a female human cadaver (Ackerman et al., 1995; Lindberg and Humphreys, 1995; Spitzer et al., 1996). These data make it possible to resolve the bodies in true colour volume elements (voxels), so that any plane through them can be visualised with high resolution. The same anatomical structures can therefore be studied indefinitely and from any direction. The Visible Human data have been utilised to clarify anatomical issues of relevance to the thesis.

1.3.2 Back extensor muscle lever arms

Lever arms of the back extensor muscles have been measured about different anatomical points, like the centre of rotation for lumbar motion segments (Macintosh et al., 1993; Bogduk et al., 1992), or the centroid of lumbar discs (McGill, 1988). Any set of forces can be reduced to one torque and one resultant force acting at any optional point. The torque will, however, depend on the point chosen. Since earlier studies do not incorporate torque contributions from the often considerable resultant force created by disc pressure, it seems that the implicit assumption has been that the disc pressure should not contribute to the torque. *In vitro* measurements have shown a rather evenly distributed disc pressure in healthy discs (McNally and Adams, 1992). The centre of pressure on a transverse disc section through the middle of the disc is thus going to be located close to the centroid of the section. This centroid therefore seems as a reasonable choice of point for evaluating the torque. For brevity, this point will henceforward simply be referred to as the disc centre.

The length of the lever arms for the different muscles around the lumbar spine has been measured on cadavers (Dumas et al., 1991) and by means of computer-assisted and magnetic resonance tomography in several studies (e.g. Thorstensson and Oddsson, 1982; Nemeth and Ohlsen, 1986; Reid et al., 1987; Kumar, 1988; McGill et al., 1988; Chaffin et al., 1990). Most of these studies have, however, examined the muscles in a gross way rather than determining the geometry and lever arm lengths for the individual fascicles of the muscles. The possibility to change the back extensor muscle lever arm lengths by voluntary changing the degree of lumbar flexion-extension has also not been considered.

1.3.3 Intra-abdominal pressure

During back extension tasks, such as lifting, there is a considerable increase in IAP (e.g. Bartelink, 1957; Davis, 1956; Morris et al., 1961). It has been proposed that the IAP can contribute to back extensor torque production and unloading of the spine (Bartelink, 1957). The first hypothesis, put forward already in the early 20's (Keith, 1923) and later corroborated by others (e.g. Bartelink, 1957; Morris et al., 1961), implied that the IAP would act to reduce the compressive load on the lumbar spine by pressing upwards on the rib cage. This proposed unloading effect of IAP has later been questioned by McGill and Norman (1987b). They stated that the possible unloading effect on the spine by an increased IAP would be counteracted by an equally large or even larger loading effect by the activated abdominal musculature with a line of pull parallel with the spine.

Already Bartelink (1957) realised that activation of the abdominal muscles could counteract the unloading effect of the lumbar spine by the IAP. Longitudinal tensions in the abdominal wall would create both a compressive force on the spine and a flexor moment, which

would need to be counteracted by an additional moment produced by increased back extensor muscle force. Bartelink used surface electromyography (EMG) to record muscular activity from the abdominal wall. His recordings showed an absence of EMG activity in rectus abdominis during lifting, whereas electrodes placed laterally to this muscle showed activity (overlying the obliquus abdominis externus and internus as well as the transversus abdominis). In his paper, Bartelink suggested that the transversus abdominis muscle should be the main abdominal muscle responsible for the increase in IAP. This hypothesis was based primarily on the anatomical arrangement of the transverse muscle, with muscle fibres running mainly in the transverse plane, thus allowing for compression of the abdominal cavity, and an IAP increase, without creating any longitudinal tension.

Both Morris et al. (1961) and McGill and Norman (1987b) have later estimated the magnitude of abdominal muscle forces from EMG recordings. Their calculations of the net effects of the IAP on the lumbar spine are contradictory. While Morris et al. arrive at a reduction of approximately 30% of lumbar spinal compression due to the IAP, McGill and Norman state that "compressive forces generated by the abdominal wall musculature were larger than the beneficial action of those forces thought to alleviate spinal compression via IAP". These discrepancies are, at least partly, due to the lack of a clearly defined model of the IAP effects. One critical variable that is poorly defined in both studies is the length of the lever arm for the IAP generated force on the diaphragm. Other reasons for the diverging conclusions may be related to methodological differences in obtaining and interpreting the EMG as well as in converting the EMG to force. It seems highly unlikely that it has been possible in these studies, both using surface EMG electrodes, to separate the action of the two oblique muscles and the transverse abdominal muscle. Cresswell et al. (1992) performed intra-muscular recordings from all the four abdominal muscles during isolated back extensions and lifting tasks. Some EMG activity was present in the obliquus internus muscle, whereas both obliquus externus and rectus abdominis in most cases were silent. However, a marked activation of the transversus abdominis accompanied the increase in IAP, thus confirming the assumptions made by Bartelink.

Thomson (1988) incorporated the shape of the abdominal cavity into a model of IAP induced unloading of the lumbar spine. In this model, based on elastic beam theory, he considered the abdominal wall to have a constant modulus of elasticity. However, this is clearly not applicable on muscular layers, whose capacity to withstand and develop force strongly depends on the degree of neural activation. By not clearly defining the external forces Thomson also makes the mistake of accounting for IAP generated extensor moment twice. Finally he assumes parts of the abdominal wall to be flat. This implies that the abdominal wall would be able to sustain considerable bending moments, which is not likely to be the case for muscular and tendinous layers. Due to the above stated misconceptions the main value of Thomson's article lies, not in his conclusions, but in focusing on the relation between the form of the abdominal cavity and the possibility to generate IAP induced unloading of the lumbar spine. A clearly defined model of the IAP effects is thus needed to clarify these issues.

1.3.4 Simultaneous equilibrium

Most models only consider the equations of motion for one free body, consisting of the upper body cut by a transverse incision through one lumbar level. Recently, however, the requirement for simultaneous equilibrium for free bodies created by incisions through each lumbar level during maximal static exertions in the form of pure torques has been considered (Stokes and Gardner-Morse, 1995). The study suggested that, for equilibrium reasons, many of the back

extensor muscle fascicles could not be activated fully or, more often, not activated at all when resisting the maximal possible external flexion torque applied to T12. These results were, however, not based on, or tested against, measurements of back extensor torque production, electromyographic activity or spinal posture in the modelled loading condition. Furthermore, the possibility that the equilibrium during maximal exertions would be achieved more by changes in the spinal posture leading to changes in muscle fascicle forces due to length changes than by a detailed motor control was not considered. For reasons stated in section 3.4, we consider this passive equilibrium control mechanism to be of major importance and, furthermore, that most back extensor muscle fascicles are close to fully activated during maximal static efforts. In this thesis, therefore, the equilibrium demand is utilized to test the model validity rather than to predict complex back extensor muscle coordination patterns.

1.3.5 Physiological cross-sectional area

Most recent studies measure physiological cross-sectional area (PCSA) as the quotient between total muscle volume and the mean muscle fibre length (with or without correction for pinnation angle) (e.g. Edgerton et al., 1986; Bogduk et al., 1992; Kawakami et al., 1994). This measure does not account for gradual muscle fibre force transmission to connective tissue over tapered fibre endings (Trotter, 1993; Eldred et al., 1993). Even if it should give a reasonable estimate of PCSA in theory, cadaver estimates of mean fibre length, at optimal length, for any given muscle will be needed and its accuracy and applicability to the studied subjects will set a limit to the accuracy of this method. We suggest that for muscle fascicles with parallel fibres, where all muscle fibres, but no tendon slips, pass the fascicle mid section, a better estimate for PCSA would be the mid section anatomical cross-sectional area (ACSA) perpendicular to the fibres and measured with the fibres at their optimal length. This is the method used in this thesis, except that since optimal fibre length is unknown we have simply used the fibre length in the anatomical position.

1.3.6 Maximal specific muscle tension

Estimates of maximal specific muscle tension from the literature have been used in biomechanical models of back extension in order to calculate muscle forces from measurements of muscle lengths and cross sectional areas (e.g. McGill and Norman, 1987a; Stokes and Gardner-Morse, 1995) and to test the validity of the model by comparisons of model estimates of muscle tensions during maximal exertions (Bogduk et al., 1992). There is, however, a large range of values, between 10-100N/cm^2, that all have been considered supported by *in vivo* experiments (McGill and Norman, 1987a; Stokes and Gardner-Morse, 1995). This is in contrast to *in vitro* measurements that show a much smaller variation in the maximal specific tension of human muscle fibres (e.g. Bottinelli et al., 1999; Stienen et al., 1996). The problems with *in vitro* measurements have been that, in order to keep the preparation under stable conditions, they have been done at low temperatures where the maximal tension is substantially lower than at normal working temperatures. Stienen et al. (1996) have, however, made measurements up to 30° and by extrapolation estimated the maximal tension at 35° to be about 19N/cm^2 for slow twitch fibres and, depending on myosin isoform, between 23-28N/cm^2 for fast twitch fibres. Typical standard deviations within one myosin isoform were only about 4 N/cm^2. In a later study (De Ruiter and De Haan, 2000) *in vivo* measurements of the maximal force production of adductor pollicis showed a force reduction of 79±3% as the muscle temperature was lowered from 37° to 22°. This information gives us the possibility to extrapolate from *in vitro* measurements ranging up to 22°. Using the data of Bottinelli et al. (1996) and compensating for

a swelling of 1.44 times (Stienen et al., 1996) in the skinned muscle fibres used for *in vitro* experiments we obtain mean values between 17-25N/cm^2 depending on myosin isoform (again the slow twitch fibres having the lower tension). In our view these data are more reliable than *in vivo* estimates that rely on maximal torque measurements and estimates of muscle lever arms and physiological cross-sectional areas. The possible range of maximal specific muscle tensions therefore seems to have been narrowed down to about 15-30N/cm^2, thereby offering a better basis for model validation.

1.4 THESIS OBJECTIVES

The purpose of this thesis has been to develop and evaluate a clearly defined model of lumbar back extension torque production incorporating detailed back extensor muscle anatomy, effects of IAP as well as effects of changes in the degree of flexion-extension of the lumbar spine. To that purpose the individual studies contribute as follows:

I. Investigates how changes in lumbar flexion-extension affect the lever arm lengths of the main back extensor muscles, utilising MR-imaging.

II. Develops and discusses a model of the most basic effects of the IAP on back extension torque production and spinal loading.

III. Investigates the anatomy of the lumbar erector spinae utilising the data from the Visible Human Project.

IV. Tests the modelling of the IAP effects by recording the torque produced about the lumbar spine due to IAP generated by phrenic nerve stimulation.

V. Synthesises a full model of lumbar back extension torque production and contributes new anatomical information from Visible Human and MR data and tests the model by comparing calculated and measured maximal back extensions about the lumbar spine.

2 METHODS

2.1 SUBJECTS

Twenty healthy subjects volunteered for the experiments. They were mainly staff and students from the Stockholm University College of Physical Education and Sports. All procedures were conducted according to the declaration of Helsinki and were approved by the Ethics Committee of the Karolinska Institutet. Subjects provided informed written consent prior to participation in the studies. Digital images of the two cadavers from the Visible Human Project were used for anatomical investigations. Data of subjects and cadavers are summarized in Table 1.

Table 1. Features of the subjects involved in this thesis; numbers (n) of respective sex, mean (±1SD) age, height and mass. Study II was purely theoretical and contained no subjects while study III contained image analysis of the two cadavers from the Visible Human (VH) Project.

Study	n	Age (years)	Height (m)	Mass (kg)
I	5 women	31 ± 9	1.73 ± 0.04	64 ± 3
	6 men	37 ± 10	1.85 ± 0.07	82 ± 6
II	0	-	-	-
III	VH woman	59	1.66	Unknown
	VH man	39	1.80	90
IV	5 men	34±5	1.83±0.10	80.6±8.9
V	4 men	27±3	1.90±0.07	82.5±7.6

2.2 PHYSIOLOGICAL MEASUREMENTS AND INTERVENTIONS

2.2.1 Back extensor strength

Maximal voluntary static back extension muscle strength about the L3 vertebra (study IV) and the L5/S1 disc (study V) was measured. The measurements were done with the subjects lying on their right side, their pelvises and straight legs tightly fixated to a vertical board and their upper bodies fixated to another vertical board attached to a swivel table (Thorstensson and Nilsson, 1982) (figure 2.1). The subjects were placed so that their L3 vertebrae or L5/S1 discs were located approximately over the centre of rotation of the swivel table. Force measurements were done with a strain gauge on a wire attached to the swivel table (with a known lever arm length about its centre of rotation used for calculating the torque). For static measurements the strain gauge was connected to a fixed support. During the dynamic trials the swivel table was moved at constant velocity (10º/s) by a servo-controlled motor. The initial acceleration to steady-state velocity was completed within 5º from the start position.

2.2.2 Intra-abdominal pressure

Recordings of IAP were made with a pressure transducer inserted through the nose, via the oesophagus, into the stomach (Grillner et al., 1978) (figure 2.1). During the externally evoked IAP generation (phrenic nerve stimulation, study IV) belts were applied to the abdomen and lower rib cage to restrict displacement of the abdominal contents as a result of diaphragm contraction (thus reinforcing the build-up of IAP).

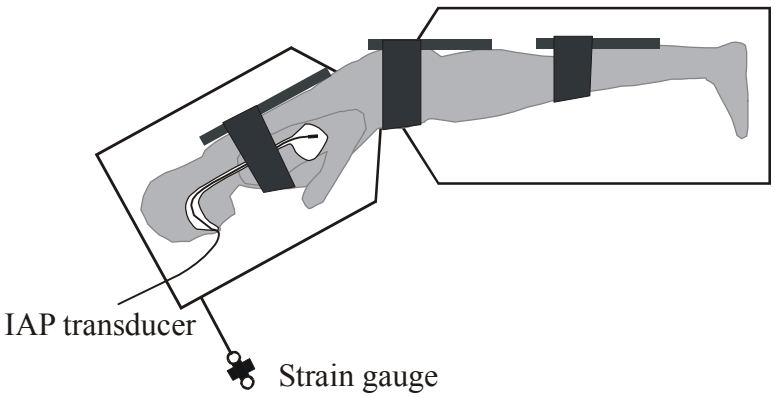

Figure 2.1. Back extensor strength and IAP measurements were performed with the subjects strapped sideways to a swivel table.

2.2.3 Electromyography

The electrical activity in the diaphragm was measured using a pair of surface electrodes placed over the chest wall (MacLean and Mattioni, 1981). The electromyographic signals were amplified 1000 times, bandpass filtered between 10-1000 Hz and sampled at 2000 Hz.

2.2.4 Phrenic nerve stimulation

Involuntary increases in IAP were produced through evoked contractions of the diaphragm by unilateral electrical stimulation of the phrenic nerve at the neck. The nerve was electrically stimulated using a probe electrode (diameter 5 mm) held manually in position, lateral to the sternocleidomastoid muscle at the level of the cricoid cartilage (Gandevia and McKenzie, 1986). The stimulating probe was positioned to produce the most selective stimulation possible without concurrent activation of the neck or shoulder muscles. Similarly, the intensity of the constant-voltage stimulus was set to achieve the highest IAP with no, or minimal, stimulation of neck or shoulder muscles (i.e. 25-50 mA). In different trials the stimulation was delivered either as a single stimulus or as a 100 ms train of 6 stimuli and 20 ms inter-pulse intervals.

2.3 ANATOMICAL ANALYSIS

2.3.1 Magnetic resonance imaging

MR imaging technique was used to study the anatomy of the abdomen and lumbar spine. Gradient echo pulse sequences in a 1 Tesla (study I) and a 1.5-Tesla (Study V) super conducting system were utilised. Images were obtained in different degrees of flexion-extension of the lumbar spine. Movements were restricted by the diameter of the camera (50 cm) so tilting the pelvis rather than moving the legs or trunk constituted most of the lumbar motion (figure 2.5). Lumbar back flexion was restricted rather by the camera diameter than by anatomical constraints, whereas the maximal lumbar back extension was not. The degree of flexion-extension was measured as the angle in the sagittal plane between the upper surfaces of sacrum and a lumbar (L) or thoracic (T) vertebra (L4 and L1 gave two angles used in study I and T11 was used to give one angle in study V). The subjects simulated static lifts during the imaging, lying supine with slightly bent hips and knees pulling with both hands on an adjustable strap fastened to a wooden bar under the feet (this arrangement made them exert force in the back extensor muscles). One transverse image through the centres of each of the lumbar discs as well as sagittal images through the middle of the spine was obtained in each trunk position. In study

V were also images obtained through the middle of the erector spine muscles on both the left and right sides (at the tips of the transverse processes). For one subject two additional sagittal images, one lateral and one medial to the mid muscle section, were obtained through the erector spinae at each side.

Measurements of muscle areas, muscle fascicle lever arm lengths as well as the geometry of the vertebral column and the abdomen (for calculations of IAP effects) were performed on the MR images. The details of these measurements are presented in section 2.4.2.

2.3.2 Visible Human data

The Visible Human Project from the US National Library of Medicine provides densely spaced transverse digital images from a male and a female human cadaver (Ackerman et al., 1995; Lindberg and Humphreys, 1995; Spitzer et al., 1996). These data make it possible to resolve the bodies in true colour volume elements (voxels), so that any plane through them can be visualised with high resolution. Both the Visible Human male and female (see section 1.1 for anthropometrical information) were selected, by the Visible Human Project, to be representative of normal human anatomy (Ackerman et al., 1995; Spitzer et al., 1996). Shortly after death they were frozen and fixated in gelatine. Transverse cryosectioning at 1 and 1/3 millimetre intervals for the male and female, respectively, was then performed and images of each section were taken. The digital images produced are in true colour (24 bits) and with a pixel spacing of 1/3 millimetre. In this thesis Visible Human data were used, courtesy of the Visible Human Project, in order to clarify anatomical information needed for the biomechanical model.

Software was produced, as part of the thesis, to visualise sections oriented in any direction and with maximum resolution. By creating adjacent images in quick succession the software allowed for free movement through the body along any route. Three-dimensional co-ordinates of anatomical structures in the images could be marked with the mouse-cursor. The quality of the Visible Human data makes it possible to clearly separate aponeurosis from muscle and also to separate the muscles erector spinae, multifidus and quadratus lumborum from each other. On the other hand, it is not possible to distinguish the borders between fascicles of the individual muscles in a single image. It is, however, possible by quickly visualising adjacent images (maximally 1 mm apart), to visually follow the muscle mass of a fascicle from rostral to caudal insertions. Within the muscle mass there is an abundance of clearly visible, local, structural irregularities (e.g. small fat deposits) spanning along the longitudinal direction of the fascicles that makes this task feasible. The fibre orientation is also clearly distinguishable when fascicles are viewed from the side. It was thus possible to define and quantify the geometry of back extensor muscle fascicles with the developed software. From this information physiological cross-sectional areas (Gans, 1982) of individual fascicles were estimated by the cross-sectional area measured in the middle of the muscular part of the fascicle in a plane perpendicular to its longitudinal orientation (inside the observed individual fascicles muscle fibres were seen to follow closely the longitudinal direction of the fascicles).

2.3.3 Dissection

Some aspects of the morphology in the Visible Human data could not be observed from the images, e.g. if two adjacent tendons were connected to each other or not. Dissection of the lumbar erector spinae of five cadavers was performed in order to clarify such qualitative matters.

2.4 BIOMECHANICAL MODELLING

2.4.1 Intra-abdominal pressure

The simplified mechanical model used to clarify some of the most basic effects of IAP is defined in the following. The walls surrounding the abdominal cavity consist of muscle and connective tissue, and can therefore not be considered being able to support bending moments to any significant degree. Loads on these walls will have to be carried by tensile and shear forces. By approximating the abdominal wall with a membrane some useful equilibrium equations can be derived. Equilibrium in the normal surface direction of the internal pressure (p) and the normal tensions (N_1, N_2) on an infinitesimal membrane element cut perpendicular to the principal axes of curvature yields equation (2.1). Here r_1 and r_2 represent the radii of curvature along the principal axes of curvature (with the exception that r will be negative along a principal axis curving away from the pressure filled membrane inside). The relation is derived in figure 2.2. The elegance of formulating the equation without reference to any specific coordinate system has been sacrificed to avoid having to introduce the rather extensive subject of tensor analysis.

$$\frac{N_1}{r_1} + \frac{N_2}{r_2} = p \tag{2.1}$$

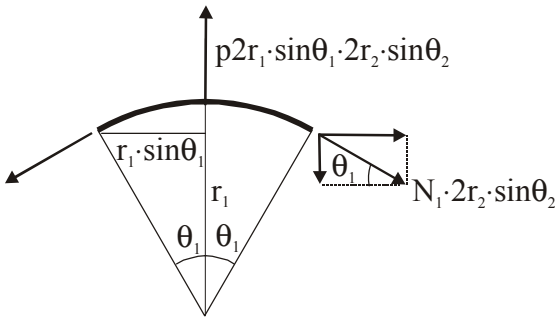

Figure 2.2. A piece of membrane cut perpendicular to the principal axes and viewed sideways from the direction of the second principal axis. Equilibrium in the normal direction (at the middle of the area segment) demands that the internal pressure (p) times the normally projected area must counteract the normal vertical components of the forces created by the tensions (N_1, N_2) at the four sides. In the limit as the area approaches zero, constant radii of curvatures (r_1, r_2) can be applied so that the equilibrium demand can be formulated as: $p2r_1 \sin\theta_1 \cdot 2r_2 \sin\theta_2 = 2N_1 r_2 2\theta_2 \sin\theta_1 + 2N_2 r_1 2\theta_1 \sin\theta_2$. Simplification of this relation and utilisation of equation (1.3) gives equation (2.1). The membrane element is cut perpendicular to the principal axes since no twisting of the membrane occurs about these axes (Aleksandrov et al., 1999), thus the shear tensions will have no component in the normal direction.

Force equilibrium in other directions gives two more independent equilibrium equations. Both these are partial differential equations. Moment equilibrium about an axis normal to the membrane yields equal magnitudes of the two shear components. For our further discussion we find it convenient to integrate the force equilibrium in the longitudinal direction over a free body consisting of a part of the abdominal cavity cut between two parallel surfaces (figure 2.3), thus yielding the equation (2.2) for the tension in the longitudinal direction ($\mathbf{N}_L$); where ds is the arc length element along the curves (c_1, c_2) encircling the transverse cuts of the abdomen.

$$\oint_{C1} \mathbf{N}_{L1} \cdot \mathbf{e}_1 ds - \oint_{C2} \mathbf{N}_{L2} \cdot \mathbf{e}_2 ds = p(A_1 - A_2) \tag{2.2}$$

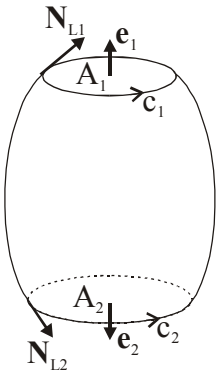

Figure 2.3. Abdominal cavity cut by two parallel surfaces. A= surface area, $\mathbf{N}_L$=normal tension, **e**=normal of unit length, c=curve surrounding surface.

Since two of the four equilibrium equations of the infinitesimal piece of membrane are differential equations, boundary values of the tension in the abdominal wall are needed in order to solve for the tension distribution. This type of information has not been available for physiological loading situations. Some simplifications are therefore needed when defining the model.

We assume the abdominal wall to be a rotationally symmetric membrane and any loading to be symmetric about the longitudinal axis. Symmetry considerations then yield constant transverse and longitudinal tension at a specific longitudinal level and zero shear tension. The abdominal wall is attached superiorly to a solid ring representing the ribs and connected to this ring is a membrane representing the diaphragm. Inferiorly the abdominal wall is attached to a circular plate constituting the pelvis with the muscles of the pelvic floor (figure 2.4). For simplicity these two circular structures will, from now on, be referred to as the rib cage and the pelvis. They are connected with a rod representing the vertebral column. The IAP generated force transmitted through the rib cage to the spine ($\mathbf{F}_{tr}$) will act at the middle of the rib cage. Force equilibrium at the rib cage yields:

$$\oint_{x=0} \mathbf{N}_L \cdot \mathbf{e}\, ds = p\pi r(0)^2 - F_{tr} \tag{2.3}$$

We let the transmitted force be expressed as the pressure times part of the rib cage area ($F_{tr} = p\pi R^2$), explicitly indicating its relative fraction of the total IAP created force on the rib cage ($F_{IAP} = p\pi r(0)^2$). Note that the value of R depends on the total effect on the rib cage, from both IAP and the longitudinal tension in the abdominal wall at the insertion to the rib cage. Equations (2.2) and (2.3) then give the longitudinal tension:

$$\begin{aligned} & p\pi r(0)^2 - p\pi R^2 - \frac{N_L(x)}{\sqrt{\frac{dr}{dx}(x)^2 + 1}} 2\pi r(x) = p(\pi r(0)^2 - \pi r(x)^2) \\ & \Rightarrow N_L(x) = \frac{p(r(x)^2 - R^2)}{2r(x)} \sqrt{\frac{dr}{dx}(x)^2 + 1} \end{aligned} \tag{2.4}$$

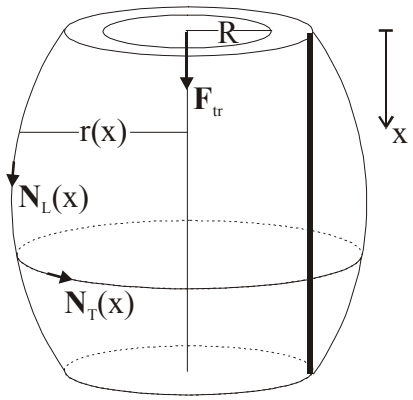

Figure 2.4. A model of the abdomen surrounded on the sides by a rotationally symmetric abdominal wall, above by a circular rib cage and below by a circular pelvis. A thick vertical line indicating the spine connects the rib cage and pelvis. $\mathbf{F}_{tr}$ = force transmitted through the rib cage to the spine. R = radius of the circle, the area of which times the IAP equals F_{tr}. r = radius of the abdominal wall about the centre line between the rib cage and pelvis. x =coordinate along the centre line between the rib cage and pelvis, x=0 at the rib cage. $\mathbf{N}_L$, $\mathbf{N}_T$ = longitudinal and transversal tensions in the abdominal wall.

Here it has been utilised that the scalar product of the longitudinal tension and the vertical unit normal equals the size of the longitudinal tension projected in the vertical direction:

$$\mathbf{N}_L \cdot \mathbf{e} = N_L \cdot \frac{dx}{\sqrt{dr^2 + dx^2}} = \frac{N_L}{\sqrt{(\frac{dr}{dx})^2 + 1}} \tag{2.5}$$

Because of the rotational symmetry, the longitudinal and transversal directions will coincide with the principal axes of curvature. Equation (2.1) can therefore be expressed along these directions:

$$\frac{N_T(x)}{r(x)\sqrt{\frac{dr}{dx}(x)^2 + 1}} + \frac{N_L(x)}{\rho(x)} = p \tag{2.6}$$

Here Meusniers's theorem (Aleksandrov et al., 1999) has been used for expressing the principal radius of curvature in the transverse direction. The principal radius of curvature (with the sign modification to fit equation (2.1)) in the longitudinal direction is defined by equation (2.7) (Aleksandrov et al., 1999).

$$\rho = -(\frac{dr}{dx}^2 + 1)^{3/2} / \frac{d^2 r}{dx^2} \tag{2.7}$$

Equation (2.4) and (2.6) can now be used to calculate the transverse tension for a given abdominal form and a given F_{tr} relative to the total IAP generated force on the rib cage:

$$N_T(x) = pr(x)\sqrt{\frac{dr}{dx}(x)^2 + 1}\left[1 - \frac{(r(x)^2 - R^2)\sqrt{\frac{dr}{dx}(x)^2 + 1}}{\rho(x)2r(x)}\right] \quad (2.8)$$

Thus, for a given IAP and a given shape of the abdomen equation (2.4) and (2.8) will yield the tensions in the abdominal wall. The solution will, however, also depend on how much of the IAP force is transmitted to the spine (via the constant R).

2.4.2 The back extension model

A model of back extension was developed, taking into account both the latest knowledge of back extensor muscle anatomy and IAP effects. The lumbar part of the erector spinae was modelled according to the anatomical description of study III while the thoracic part was modelled according to Bogduk et al. (1992) and Macintosh and Bogduk (1987). For the lumbar multifidus the description of Macintosh and Bogduk (1986) was used and for quadratus lumborum standard textbook descriptions were utilised (Williams et al., 1995). The anatomical descriptions of multifidus and quadratus lumborum were both confirmed by our own observations of attachments on the Visible Human male. For the anatomy of the thoracic multifidus we solely relied on observations of the Visible Human male (as presented in study V).

For each subject the geometry of the lumbar back extensor muscles as well as the geometry of the lumbar spine and the pressurised column generated by the IAP were measured on the MR-images. The coordinates for the insertions of individual muscle fascicles were located and the fascicles were assumed to run in straight lines between these insertions. The exception was the thoracic part of the lumbar erector spinae that at least in the flexed position must follow a curved path along the convex rib cage. These fascicles were assumed to transmit their force through the erector spinae aponeurosis just rostral to the aponeurotic attachments for the lumbar part of the lumbar erector spinae. Lever arm lengths for the muscle fascicles about the lumbar disc centres in the sagittal plane were then calculated from the measured coordinates. Measurements from the Visible Human male and female showed that the centroid of a mid transverse lumbar disc section is situated close to the mid point between the anterior and posterior border of the disc in the mid-sagittal plane. The mean discrepancy was 0.9 mm and the differences were never greater than 2.2 mm. Since the mid point in the sagittal plane is more reliably obtained from the MR images, this point was chosen as the moment point.

The physiological muscle cross-section areas of the muscle fascicles were measured in the Visible Human male for all muscles except the thoracic part of erector spinae that was estimated according to Bogduk et al. (1992). For reasons stated in the Background (section 1.3.5), the largest anatomical cross-sectional area perpendicular to the fascicles' longitudinal direction was used as the physiological cross-sectional area (PCSA). Scaling factors to calculate absolute values for the individual subjects were calculated as the quotient of the transverse muscle cross sections through the L3/L4 level on the MR-images (taken in a posture with similar spinal curvature as the Visible Human male) and through the same level in the Visible Human data. Measurements and scaling factors were obtained separately for the lumbar erector spinae, multifidus and quadratus lumborum. For the thoracic erector spinae the PCSA was assumed to have the same scaling factor as that which the lumbar erector spinae from Bogduk et al. (1992) would need in order to equal our estimates.

Since information about sarcomere lengths and reliable values of average muscle fibre lengths for the different back extensor muscles in a given position is missing it is not possible to model the variation of specific tension as a function of length of individual muscle fascicles. As a first approximation, for any given lumbar position, we therefore assumed the same specific tension for all fascicles.

As a first approximation we assumed all the back extensors to be equally activated during maximal exertions. The study by Stokes and Gardner-Morse (1995) discussed in section 1.3.4 seemed to indicate the opposite, that there would have to be a large variation in fascicle activation. There are, however, several reasons for believing this not to be the case. Information about the detailed back extensor muscle activity during back extension efforts is sparse but points to gross muscle activity rather than independent fascicle activation (Jonsson, 1970). Simply palpating the back during maximal back extension does not reveal the kind of coordination pattern (with a mixing of fully activated and totally relaxed fascicles) suggested by Stokes and Gardner-Morse (1995), instead all fascicles palpable are highly tensed. The amount of neural substrates, from spinal grey matter to motor cortex, controlling the back extensor muscles is also much smaller compared to the substrates controlling body parts with a high degree of independent muscle fascicle activation, as for instance the hand. Finally, if there were a significant amount of fascicles that could not be activated close to their maximum, it would imply even larger maximal specific muscle tensions for the back extensor models. In fact, these models already tend to overestimate the maximal tension as compared to *in vitro* measurements. In our view it is, therefore, most likely that the back extensor muscles to a large degree are close to maximally activated during maximal static back extension.

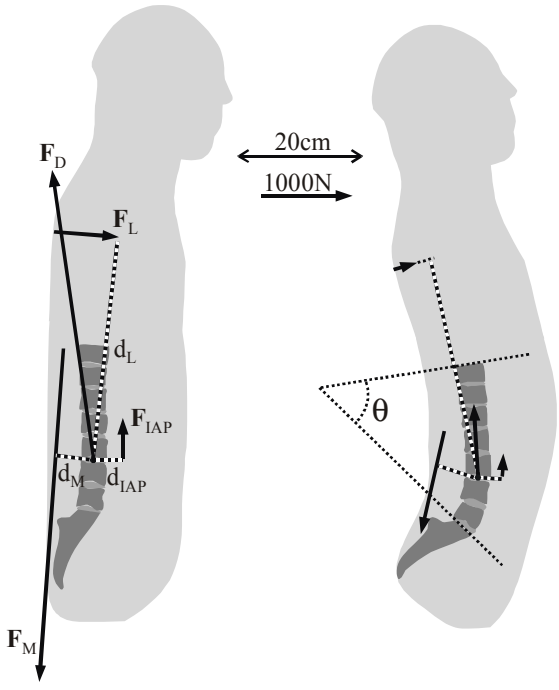

Figure 2.5. The lower spine (from T11 to sacrum) and the upper body of one subject drawn from the MR-images taken in the most flexed (left) and the most extended position. The T11-S1 angle (θ) is marked in the drawing of the extended position. The external forces (**F**) acting on a free body diagram of the upper body cut at the L3/L4 disc and their lever arms (d) about the point of application on the disc contact force have been drawn. The forces and lever arms correspond to group mean values for the respective position (study V). $\mathbf{F}_D$=resultant disc contact force, $\mathbf{F}_M$=resultant back extensor muscle force, $\mathbf{F}_L$=external load, $\mathbf{F}_{IAP}$=intra-abdominal pressure force. Calibration bars for distance and force are given between the drawings.

Conclusions drawn from the IAP model of section 2.4.1 guided the incorporation of IAP effects in the back extension model. In the transverse MR-images the spine, the quadratus lumborum, the transversus abdominis and rectus abdominis surrounded the abdominal cavity. It was assumed that a uniform IAP acted here. For each lumbar level the IAP area and its centre of pressure were measured. The IAP was modelled to act as a pressurised column transmitting force between the rib cage and the pelvic floor. The line of force was assumed to act along the average line through the centre of pressures over the different lumbar levels. The cross-sectional area of the column was defined as the smallest cross-sectional area from the transverse MR-images, corrected to represent an area perpendicular to the line of force. Lever arm lengths for the IAP force about the lumbar disc centres were also calculated.

No torques were assumed to be created about the selected moment points by forces in the discs and facet joints. The external force on the back during the strength measurements was assumed to act perpendicular to the board supporting the back.

The equilibrium of the upper body cut transversally through given lumbar levels was considered. Figure 2.5 shows the external forces acting on the free body cut through the L3/L4 level, during maximal voluntary back extensions.

2.4.3 Model validation

The model has been tested in three ways. Firstly by comparing the back extension torque created by involuntary IAP activation (section 2.2.4) with model estimates. Secondly by comparing how well the specific muscle tension needed to obtain the maximal torques from the strength measurements corresponded to estimates of human maximal specific muscle tensions from the literature (see section 1.3.6). Thirdly by analysing how well simultaneous equilibrium can be generated during the maximal static back extensions, for free body diagrams of the upper body, transversely cut through each lumbar disc.

2.5 STATISTICS

Arithmetic mean has been used as a measure of central tendency and standard deviation as a measure of dispersion. Paired two-tailed t-tests, with a significance level of $p<0.05$, were used to judge statistical significance. Pearson's correlation coefficient (r) was used to evaluate linear correlations between variables.

3 RESULTS AND DISCUSSION

3.1 BACK EXTENSOR MUSCLE ANATOMY

The detailed anatomy of the lumbar part of the lumbar erector spinae was derived from the Visible Human male and female. In accordance with Bustami (1986) but contrary to Macintosh and Bogduk (1987) it was found that the muscles do attach caudally to the erector spinae aponeurosis (ESA) (figure 3.1 for the male and figure 3 and 4 in study III for the female). This implies a different muscle geometry than that used in earlier detailed back extension models (e.g. Bogduk et al., 1992; McGill and Norman, 1987a; Stokes and Gardner-Morse, 1995).

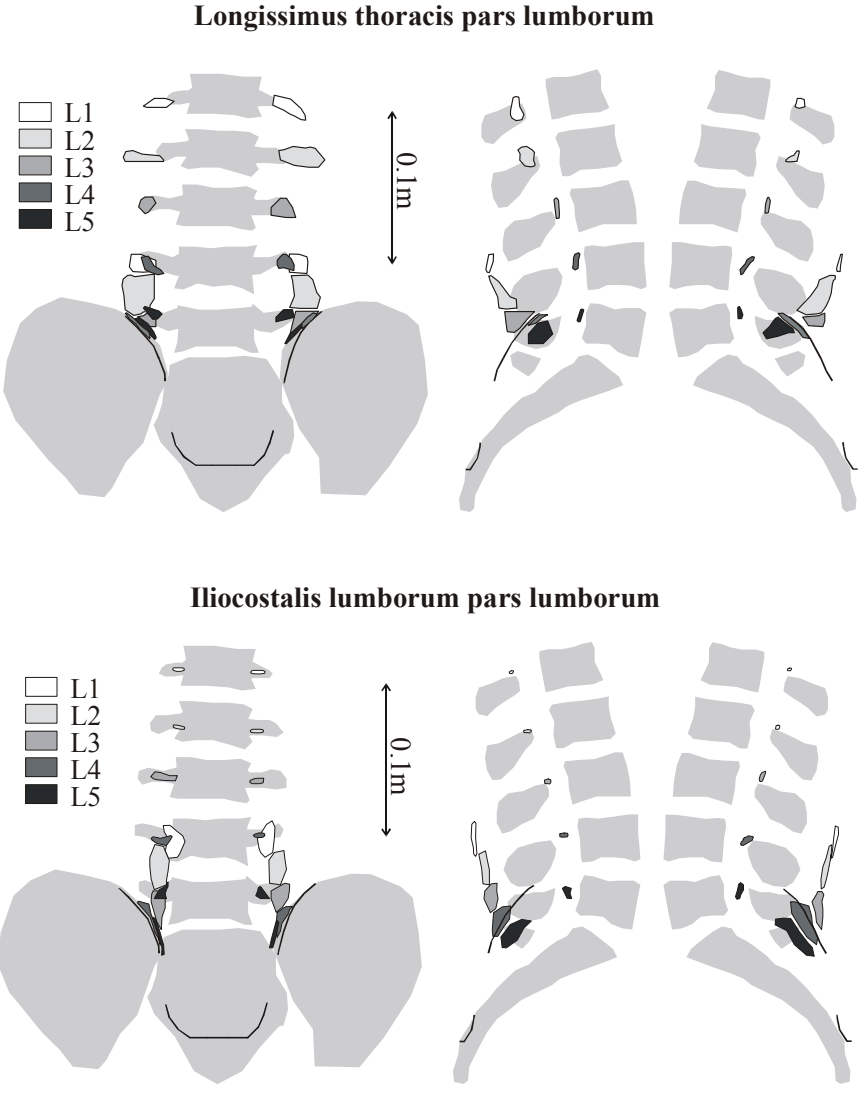

Figure 3.1. Approximate rostral and caudal attachments of the lumbar part of longissimus thoracis (above) and iliocostalis lumborum (below) for the Visible Human male. From left to right are views from the rear and from the right and left sides, respectively. Muscle fascicles are marked with a greyscale according to their rostral attachment (see insets to the left). The attachments of the erector spinae aponeurosis on the iliac crest and sacrum are marked with black lines.

Divisions and denominations of the muscles are in one sense only a matter of definition. Logical denominations, with unambiguous borders between different divisions, are, however,

desirable. The Visible Human data do not allow a clear separation of the erector spinae originating from the lumbar levels into a medial and a lateral part solely by their rostral attachments. It is, however, to some degree possible to make such a division based on the caudal attachments in relation to the lumbar intermuscular aponeurosis (LIA). As Bogduk and Macintosh describe (Macintosh and Bogduk, 1987; Bogduk, 1980), correspondence between the attachments of the thoracic and the lumbar fascicles makes it reasonable to view the lumbar fascicles with caudal attachments through or medial to the LIA as part of longissimus thoracis and fascicles with attachments lateral to the LIA as part of iliocostalis lumborum. Fascicles from the L5 vertebra were not separated by the LIA. We still chose to view the lateral fascicles as part of iliocostalis lumborum. This is based on their rostral attachments to the tips of the transverse processes, which were consistent with the iliocostalis thoracis fascicles from the other lumbar levels.

With the above stated denomination the anatomy can be described as follows. Longissimus thoracis pars lumborum attaches rostrally to the accessory processes and the medial part of the transverse processes of the lumbar vertebrae (figure 3.1). The fascicles from the three superior lumbar vertebrae (L1, L2 and L3) attach caudally to the ESA while the fascicles from the two most caudal vertebrae (L4 and L5) insert directly to the medial part of the iliac crest and on the posterior-superior iliac spine. The lateral parts of the fascicles from the L1-L4 vertebrae become tendinous inside the muscle, constituting the thin LIA. This aponeurosis merges caudally to the ESA except for the part originating from the L4 fascicle that attaches directly to the posterior-superior iliac spine.

Iliocostalis lumborum pars lumborum attaches rostrally to the lateral part of the transverse processes of the lumbar vertebrae and the adjacent surface of the middle layer of the thoracolumbar fascia (figure 3.1). The rostral attachments to the thoracolumbar fascia are most prominent at the level of the L1 and L2 vertebrae extending up to 3 cm laterally from the tips of the transverse processes. At more caudal levels the attachments to the thoracolumbar fascia become smaller, disappearing entirely for the fascicles from the L5 vertebra. Caudally the fascicles from the L1 to L3 vertebrae attach to the ESA, just laterally to the fascicles of the longissimus thoracis from corresponding levels. Fascicles from the L4 and L5 vertebrae have caudal attachments directly to the iliac crest. The reason that we, unlike previous studies, found iliocostalis lumborum fascicles from L5 might be that the Visible Human cadavers are younger than the average cadavers studied in dissection studies. These fascicles might degenerate with age. In line with this we saw much more fat tissue in the L5 fascicle of the older female Visible Human cadaver than in the male. The physiological cross-sectional (PCSA) areas of the individual fascicles of the longissimus thoracis and iliocostalis lumborum are presented in study III (tables 1 and 2).

Analysis of the anatomy of the Visible Human male thoracic multifidus showed an organisation in principle like the one for lumbar multifidus (Macintosh and Bogduk, 1986). Measured PCSA of individual fascicles are presented in study V (table 1). Visible Human analysis of quadratus lumborum showed no large deviations from standard textbook description. The PCSAs of its individual fascicles are presented in study V (in the Results text).

Since the present description of the lumbar erector spinae deviates from previously often referenced cadaver studies (Macintosh and Bogduk, 1987; Bogduk, 1980) one can reflect on how much this description is representing human anatomy from a general point of view. This interpretation will depend largely on the degree of inter-individual variability. Both the Visible Humans (and the cadavers studied) showed principally similar anatomical arrangements. The observed attachments to the ESA were in agreement with Bustami (1986). By themselves our observations are, of course, too few for generalizations. However, that an inter-individual

variability would account for the earlier described considerable and consistent differences between studies becomes unlikely considering that only small inter-individual differences have been reported in earlier studies (Macintosh and Bogduk, 1987; Bogduk, 1980; Bustami, 1986). In accordance with this Macintosh and Bogduk (1991) also explicitly state that the attachments of the individual fascicles of the lumbar erector spinae in their studies were highly clustered and showed little variation between cadavers. It is therefore our belief that differences between studies to a large part have methodological causes rather than being due to large individual anatomical variations in the examined cadavers. Considering the dissection techniques used by Macintosh and Bogduk (1987) it could be suspected that they have surgically partitioned the firm mechanical connections (as we have observed in the studied cadavers) between the ESA and the caudal tendons of the lumbar part of the lumbar erector spinae muscles.

The intrinsic muscles of the lumbar spine have not been incorporated in the model but their characteristics have been quantified. Averaged over all lumbar spinal levels and both sides of the Visible Human male the unilateral physiological cross-sectional area of the lumbar interspinales fascicles was 79±6 mm^2 and the area of the lumbar intertransversarii 126±53 mm^2 (with an upper range of 199 mm^2). With lever arms of approximately 5 cm and 3 cm, respectively, these muscles together can maximally generate an extensor torque of approximately 5 Nm at each lumbar level. Thus, the magnitude of the relative contribution to the total maximal torque would not be greater than 3% at any lumbar level.

Studying the newly available data from the Visible Human Project has some advantages over dissection studies. Uncovering a structure in a dissection often implies destroying others thereby limiting the possibility to re-examine the structure from different directions. Quantifying observations during dissection can also be problematic. With the Visible Human data, on the other hand, structures of interest can be studied from many different directions and the same data can be analysed indefinitely, e.g. by different groups. It is also much easier to quantify geometric information since all image data are fixed in a well-defined co-ordinate system. Another advantage is that the Visible Human cadavers have been selected to represent a healthy anatomy. They were also frozen shortly after death, preventing any deterioration of the organs. The Visible Human data clearly expand the possibilities for anatomical investigations, but they also have some obvious limitations. There are, at present, only two cadavers available. In addition, some aspects of anatomy cannot be investigated from images alone, e.g. if two structures are connected or just lie adjacent to each other. Dissections will therefore be a necessary complement to “Visible Human” studies.

3.2 INTRA-ABDOMINAL PRESSURE

Analysis of the IAP model of section 2.4.1 shows that the net effect of the IAP and the tension in the abdominal wall needed to generate the IAP can generate back extension torque and unload the lumbar spine during back extensions. The unloading mechanism can be viewed as a pressurised column tending to push the rib cage and pelvis apart. Longitudinal tension pulling the rib cage and pelvis together will reduce the area of the effective pressurised column while the opposite is true for any tension pulling the rib cage and pelvis apart. The latter occurs when the abdomen is bulging up beyond the rib cage and down beyond the pelvis (figure 3.2c). The maximal possible cross-sectional area of this column cannot exceed the smallest abdominal transverse cross-sectional area (figure 3.2). Otherwise, as can be seen from equation (2.4), the longitudinal tension in the abdominal wall at the level of the smallest cross section would have to become negative (i.e. changing direction to compression), which, to any significant degree, would be impossible for a sheet consisting of muscle and tendon. The notion of a pressurised

column can be generalised so that it applies to general forms of the abdominal cavity. The column should then be defined as the sum of all parallel infinitesimal straight columns connecting the rib cage and pelvis. Only through such a column can an IAP generated force be transmitted past the lumbar spine. The pressurised column generates an average force interaction between the pelvic floor and the ribcage that is oriented along a line through the columns' centres of pressure in the transverse planes. Magnetic resonance images of the subjects in study V show that this force has a lever arm length of approximately 5 cm for extension about the lumbar disc centres (figure 5 of study V) and that the maximal possible area of the pressurised column is approximately 200 cm^2 (figure 3.5). With these values and an IAP of 15 kPa (typical value measured during the maximal voluntary back extensions of study V, figure 3.5) the IAP generated back extension torque would equal 15 Nm. This is just to give the order of magnitude. For the torque created about the L5/S1 level the individual variation as well as the variation due to changes in flexion-extension are indicated in figure 3.4. IAP generated torques about more rostral disc centres will tend to be smaller due to shorter lever arm lengths for the IAP (figure 5 of study V). Still, about every lumbar level and in every individual case the IAP did generate back extension torque. During back extensions the pressurised column will unload the lumbar spine both directly by pressing the rib cage and pelvis apart and indirectly by producing a back extension torque which, for a given total torque requirement, reduces the need for back extensor muscle force. The size of the direct and indirect unloading will be of the same order of magnitude, since the IAP and back extensor muscle lever arms are of similar size (figure 5 of study V). With the above mentioned typical values of IAP and its effective cross-sectional area the order of magnitude of the spinal unloading would be 600N.

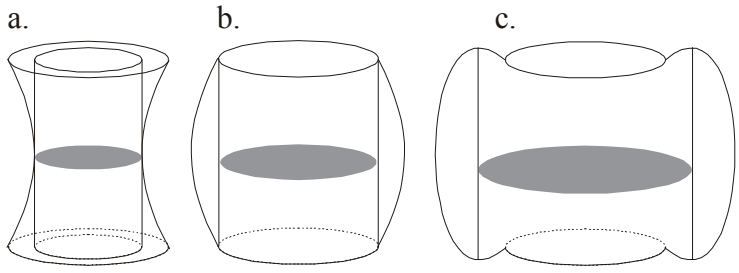

Figure 3.2. The maximal possible cross-sections of the pressurised columns between the rib cage and pelvis for three different forms of the abdominal wall.

Now let us consider how the shape of the abdomen will affect the possibility to generate IAP and IAP induced unloading of the lumbar spine. Equation (2.1) shows that, in order to withstand internal pressure, a membrane needs a non-zero curvature (non-infinite radius of curvature) and a non-zero tension in at least one direction. Since we assume the abdominal wall as being incapable of carrying compressive loads, this curvature needs to be directed inwards towards the pressurised side of the membrane (i.e. like a balloon).

The diaphragm, the abdominal wall and the pelvic floor will have to withstand the same pressure (disregarding gravity which produces a small pressure gradient of around 0.1 kPa/cm in the vertical direction). The maximal IAP will then be restricted by the structure with the lowest pressure producing capacity. This capacity will, however, vary with the length of the fibres in the muscle sheets. A shortening will reduce the pressure producing capacity by reducing the curvature and, most likely, also the maximal tension producing capacity based on the basic length-tension relationship for muscle fibres (Gordon et al., 1966). Since the abdomen

can be considered as incompressible we can assume it to have a more or less constant volume (except for blood that can be pressed out). A shortening of one muscle sheet will therefore demand a lengthening somewhere else in order to maintain the volume. An optimal form for maximal IAP production will accordingly be one where the diaphragm, the abdominal wall and the muscles of the pelvic floor have adjusted their lengths so that all three have the same pressure producing capacity. From this we understand that there will be a limit as to how much the abdomen can bulge out while still producing a substantial IAP. The limitation for pressure production lies, in that case, in the diaphragm (and pelvic floor) rather than in the stretched abdominal wall.

A large IAP is, as such, not a sufficient prerequisite for IAP induced unloading of the lumbar spine. As discussed earlier, longitudinal tension in the abdominal wall can counteract the beneficial effects of the IAP by pulling the rib cage and pelvis towards each other and thereby reducing the area of the effective pressurised column. This can be avoided by utilising only transverse tension in the abdominal wall to generate the pressure. Such a strategy is a likely candidate for a physiological tension distribution and would lead to a cylindrical abdominal form. As discussed in further detail in study II, longitudinal tension could be beneficial if the abdominal wall by bulging out heavily is pulling the rib cage mainly straight forward or even upwards (as in figure 3.2c). Since such abdominal forms rarely are observed in real life it appears unlikely that they are beneficial within the normal physiological range. From simple observation of the abdominal form during back extensions, it seems that the curvature in the transverse direction is much larger than that in the longitudinal direction. Intramuscular EMG recordings from all the abdominal muscles during back extension have shown a marked activation of the transversus abdominis and some activity in the obliquus internus (Cresswell et al., 1992). This activation pattern indicates a tension distribution with mainly transverse tension in the abdominal wall. It is therefore likely that a cylindrical abdominal form is a reasonable first approximation of a physiological strategy, although it is by no means an absolute prerequisite for IAP induced spinal unloading.

The cylindrical form has some important advantages in generating IAP related unloading of the lumbar spine. Longitudinal tensions, which can counteract the IAP generated unloading, are not needed. Therefore, the whole rib cage and pelvic areas can be utilised in the effective pressurised column. As compared with a more out-bulging abdominal form the diaphragm will have a greater IAP producing capacity since its fibres will be elongated and its curvature increased. For the IAP producing capacity of the transverse fibres in the abdominal wall the advantage is not so evident, since they will have greater curvature but shorter lengths. Equation (2.4) and (2.8) yield the tensions for a cylinder with radius r:

$$N_L = \frac{p(r^2 - R^2)}{2r} \tag{3.1}$$

$$N_T = pr \tag{3.2}$$

It is evident that the longitudinal tension reduces the area of the pressurised column and that it does not assist the transverse pressure in creating IAP. Thus, from a functional point of view such a longitudinal force should be avoided, that is muscles with a mainly longitudinal orientation are not suitable for IAP induced spinal unloading for a cylindrical form of the abdomen. Still, a component of longitudinal tension will be present if the transversal tension is produced by fibres in the abdominal wall with an oblique orientation, such as the obliquus

internus and externus (figure 3.3). Tension in fibres with an inclination (θ) to the longitudinal direction will increase longitudinal and transversal tension as follows:

$$\Delta N_L = N_f \cos^2\theta, \quad \Delta N_T = N_f \sin^2\theta \tag{3.3}$$

Pressure will therefore increase according to the following equation:

$$\Delta p = \frac{N_f \sin^2\phi}{r} \tag{3.4}$$

In order to utilise the tension in fibres of θ inclination for unloading the lumbar spine, the beneficial effects of increasing the pressure need to be greater than the negative effects due to the increased longitudinal tension:

$$\Delta p \cdot \pi r^2 > \Delta N_L \cdot 2\pi r \;\Rightarrow\; N_f \sin^2\theta \cdot \pi r > N_f \cos^2\theta \cdot 2\pi r \;\Rightarrow\; \theta > \text{atan}(2^{1/2}) \tag{3.5}$$

In other words, fibres with inclinations greater than approximately 55° versus the vertical will contribute to unloading, while tension in fibres of an inclination smaller than 55° instead will load the spine. Pure transverse tension will, however, be most effective. We therefore postulate that only the transverse muscle be activated during submaximal contractions while muscles with more oblique fibres will contribute in efforts closer to the maximum.

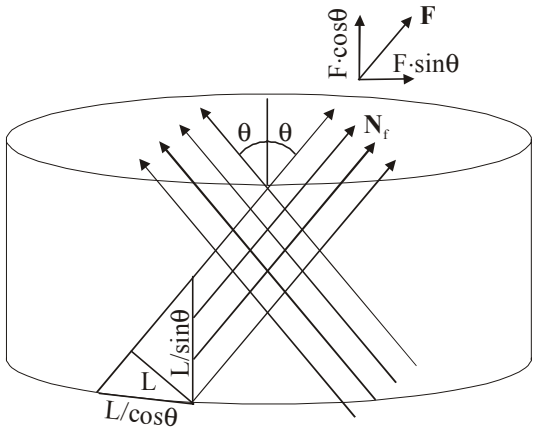

Figure 3.3. Cross-section of a cylindrically shaped abdomen with force carrying fibres inclined (θ) to the longitudinal direction. **F** = force in a fibre, $\mathbf{N}_f$ = fibre tension, L = distance perpendicular to the fibre orientation. The tension in the longitudinal and transversal direction will vary as a function of θ according to both the changing components of **F** and the changing number of fibres per cross-section in the respective direction.

The rotationally symmetric model reveals some important benefits in having a cylindrical abdominal form when generating IAP induced unloading of the lumbar spine. In a real human, the form will rather be that of a half-cylinder, where the spine and back extensor muscles will constitute a stiff back plate. This will not, however, change our reasoning. There will still be a large curvature in the transverse direction, no need for longitudinal tension and good conditions for the diaphragm to produce IAP.

In order for the IAP to unload the lumbar spine it has to be transmitted from the pressurised column and diaphragm through the rib cage to the spine (parts of the diaphragm

connected to the spine will, of course, transmit force directly to the spine). This may be a reason for activating intercostal muscles during lifting (Morris et al., 1961), since these muscles will stiffen the rib cage and facilitate force and moment transmission to the spine. The pressure increase in the thorax that can be generated by such muscle activation can also assist in the force transmission.

3.3 EFFECTS OF CHANGES IN FLEXION-EXTENSION

Both the force producing capability and the lever arm lengths about the lumbar discs for the back extensor muscles as well as the IAP will be affected by changes in flexion-extension of the lumbar spine. Study V measurements of isometric maximal voluntary back extension strength about the L5/S1 disc showed 2.7 times larger torques in the most flexed position as compared to the most extended position (figure 3.4). The fraction of the total torque created by the IAP (calculated from the model) constituted about 9% in the most flexed position and about 13% in the most extended position. The absolute values were, however, 1.8 times larger in the most flexed as compared to the most extended position (figure 3.4).

The reasons for the larger IAP generated torque in the flexed position are both an increased IAP and an increased area for the IAP to act upon (figure 3.5). The IAP lever arm length about the L5/S1 disc showed no significant increase for the flexed lumbar spine. It did, however, show such an increase for most of the more rostral discs (figure 5 of study V).

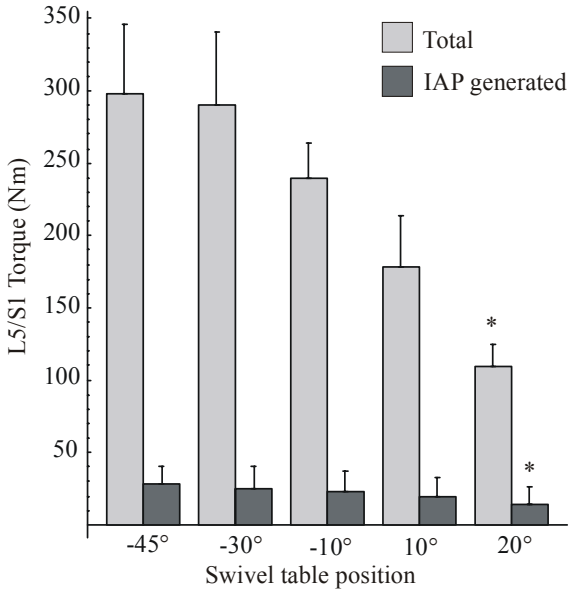

Figure 3.4. Group mean values from study V (+1SD) of measured isometric maximal voluntary strength (torque about L5/S1) and the model-calculated torque contribution from IAP in positions from 45° of flexion to 20° of extension. The asterisks represent significant differences between the most extended and the most flexed position.

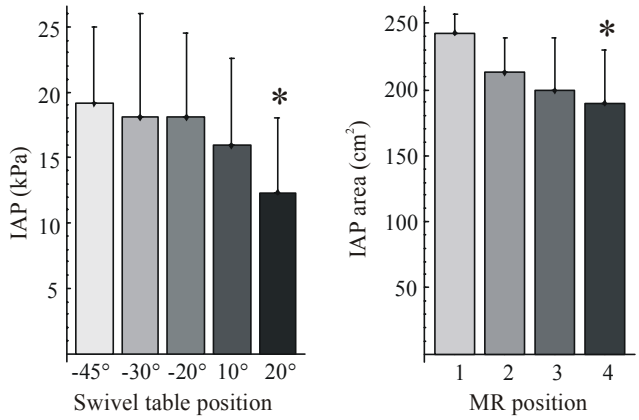

Figure 3.5. Measured group means from study V (+1 SD) of IAP during the maximal isometric back extensions and of the effective IAP area determined with MR. Both measures are presented for different degrees of lumbar back extension and flexion. The angle -45º represents the most flexed position and 20º the most extended position during the strength measurements, while position 1 represents the most flexed and position 4 the most extended position in the MR camera. The asterisks indicate significant differences between the most extended and the most flexed position.

The analysis of the MR images from study I showed that lever arm lengths for the erector spinae and the erector spinae aponeurosis were significantly longer in extension than in flexion at all lumbar levels (figure 3.6). Measurements from study V, based on detailed descriptions of individual fascicles, showed significantly longer lever arms in the extended position for all the back extensor muscles taken together as one muscle equivalent about three rostral lumbar disc centres (figure 3.7). The largest mean increase was 13.3% at the L2/L3 level, while at the L5/S1 level there was rather a tendency towards a decrease. Lever arm lengths at different degrees of lumbar flexion-extension are presented in figure 5 of study V. Since the back extensor muscle lever arm about the L5/S1 disc centre does not change markedly the main reason for the larger back extensor torques in the most flexed position (figure 3.4) must be that the muscles can create much larger forces in the flexed position, most likely due to their length-tension relationships. In absolute terms the IAP was also contributing more to the torque production in the flexed position.

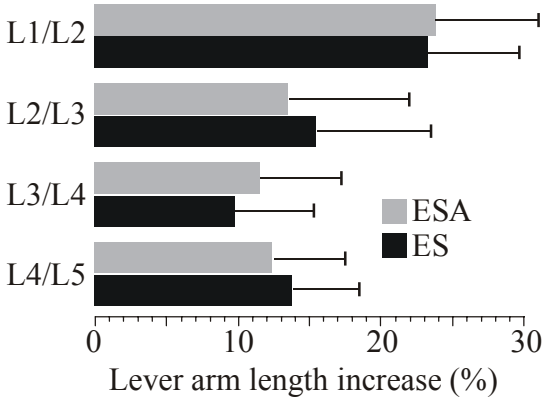

Figure 3.6. Group mean (+1 SD) percentage increase from study I of the erector spinae (ES) and the erector spinae aponeurosis (ESA) lever arm lengths at different lumbar levels comparing the extended to the flexed position. All increases were significant.

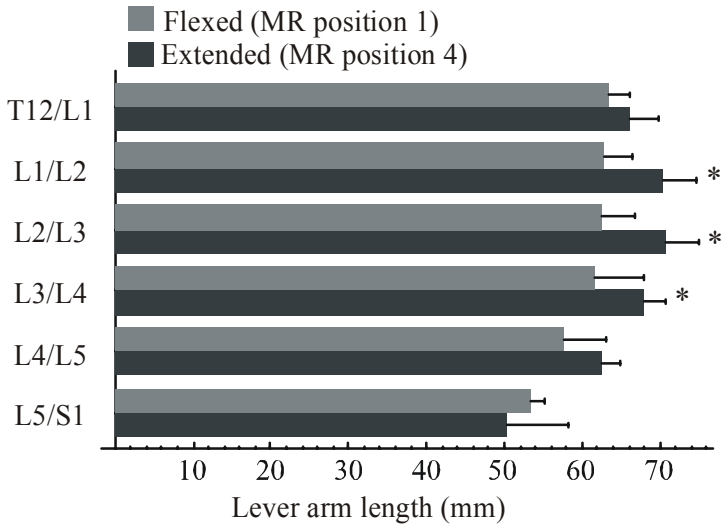

Figure 3.7. Group mean lever arm lengths (+1 SD) of the muscle equivalent for all the back extensor muscles (study V). Values are shown for both the most flexed (position 1) and the most extended position (position 4) in the MR-camera and for each lumbar level. The asterisks represent significant differences between the most extended and the most flexed position.

The model calculated disc contact forces during maximal back extensions were over four times larger in the most flexed as compared to the most extended MR position. When the torque production in the flexed position was lowered in the model to the maximal torque in the extended position (by reducing the muscle tension) there were no big differences between the contact forces in the two positions (figure 3.8), provided that the IAP still was maintained at the same level as during maximal torque production. If, however, the IAP effects were excluded the compressive forces were significantly larger in the flexed position at most lumbar levels (figure 3.8). Incorporating, rather than excluding, the IAP, significantly reduced model-calculated disc compression in all postures and at all lumbar levels. The mean reduction, rather similar for all lumbar levels, was approximately 400N in the extended position and 700N in the flexed position. During maximal back extensions this would lead to a 19-25% mean compressive load reduction in the most flexed position and a 34-40% reduction in the most extended position. The higher percentages in these ranges were found for the most rostral lumbar levels with a continuous decline caudally. In the extended position shear forces were significantly larger on the L5/S1 disc as compared to any other disc while in the flexed position there were no significant differences (figure 3.8).

It is commonly believed that safe lifting should be performed with a relatively extended lumbar spine. The increased back extensor muscle lever arm lengths with increased lumbar extension (at least in the rostral lumbar spine) offer a possible mechanical rationale for such a claim. Increased muscle lever arm lengths reduce the need for muscle force and hence the spinal loading is reduced. On the other hand increased lumbar extension also reduces the unloading effects of the IAP (by reducing the IAP, the area of the pressurised column and the IAP lever arm lengths about the rostral lumbar disc centres). The model calculations indicate that, for the extended as compared to the flexed lumbar posture, the reduced IAP unloading effect is of equal magnitude as the increased unloading effect due to changes in back muscle geometry. From a mechanical point of view it is therefore not clear that generating a given torque in an extended position will load the spine less than generating the same torque in a flexed position.

On the other hand, it is possible to generate larger absolute torques in the flexed position, which will generate larger spinal loadings. This might make flexion a more dangerous lifting posture.

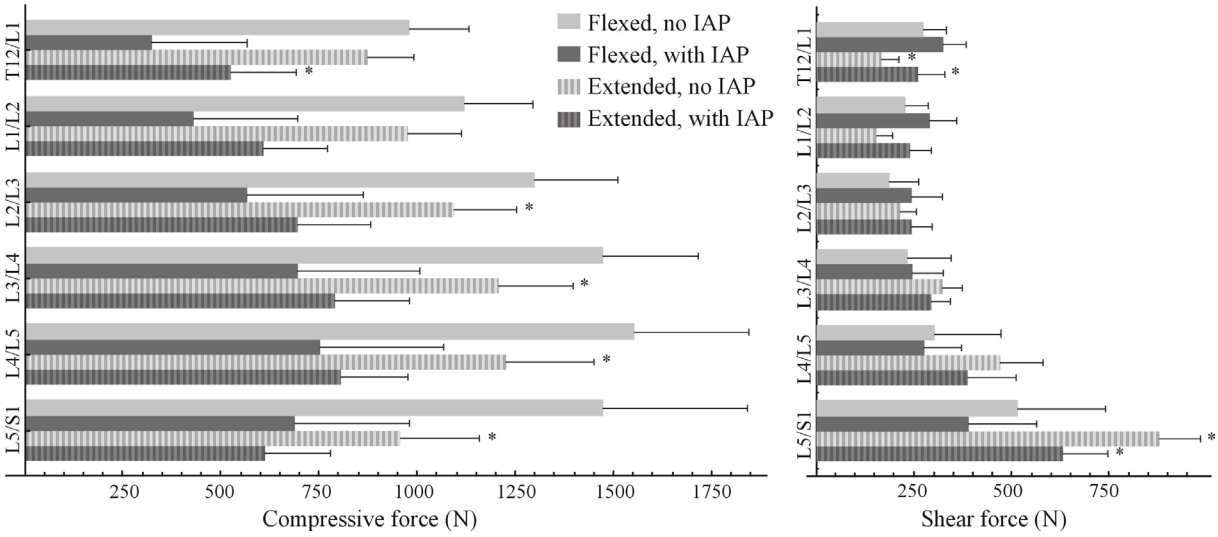

Figure 3.8. Group means (+1SD) of model-calculated disc contact forces when creating a back extension torque corresponding in size to the maximum voluntary torque in the maximally extended MR position (109.2±17.8Nm), plotted for the most extended position (MR position 4) and in the most flexed position (MR position 1). Calculations have been made both with and without IAP incorporated. With IAP incorporated, the highest IAP during maximal voluntary extension in the respective positions was utilized. The shear force acting on a transverse section of a disc is here defined to be positive when it is directed dorsally on the rostral part of the cut disc. The asterisks represent significant differences between the extended and the flexed positions.

3.4 TESTING THE MODEL

Modelling of the IAP influence on back extension torque production was tested in study IV by involuntary increases in IAP (without concurrent activation of the trunk flexor or extensor muscles) through evoked contractions of the diaphragm by unilateral electrical stimulation of the phrenic nerve at the neck. With the subjects positioned in trunk flexion (~50˚) the nerve stimulation generated a mean ± SD increase in abdominal pressure of 2.9±0.1 kPa (14.7±0.5% of that in a maximal voluntary effort). This pressure increase resulted in an extensor torque of 5.7±0.5 Nm that followed the onset of the pressure change by 34.5±0.2 ms (figure 3.9). When the amplitude of the increase in IAP was varied by stimulation of the phrenic nerve at two-thirds of the maximum intensity and using single stimuli there was a corresponding variation in the resultant extensor torque. Furthermore, the amplitude of the increase in IAP produced by the different stimuli conditions was correlated with the amplitude of the extensor torque (r=0.86, p<0.01). This finding provides support for a causal relationship between the two parameters. Measurements during isokinetic flexion (10º/s) showed similar increases in IAP and extensor torques as during the static trials. These results provided the first *in vivo* evidence of the trunk extensor torque that can be generated by an increase in IAP and they were consistent with the predictions of the biomechanical modelling.

Using the biomechanical model with measured typical values of IAP cross-sectional area and lever arm length (200 cm^2 and 5 cm, respectively), the predicted extensor torque around L3 produced by an IAP increase of 2.9 kPa (highest stimulation intensity, 100 ms train) would be 2.9 Nm. This torque is of the same order of magnitude as the torque measured *in vivo* in the

flexed position, thereby supporting the IAP modelling. This was corroborated by the extensor torques measured with the different stimulation parameters (see also table 1 of study IV).

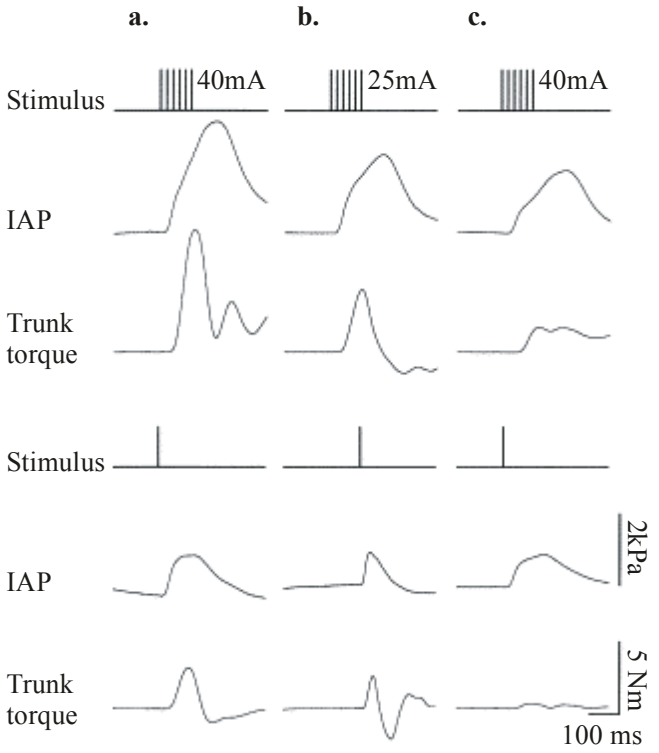

Figure 3.9. Torque resulting from electrically evoked elevation of intra-abdominal pressure (IAP). (a) IAP and torque (averaged over 10 repetitions for one subject) resulting from stimulation of the phrenic nerve (upper panels: multiple stimuli, lower panels: single stimuli) while the subject was positioned in ~50˚ of trunk flexion. A rebound of the torque resulted from the slight elasticity of the metal cable and swivel table. (b) Average data for one subject for stimuli delivered at approximately two-thirds of the stimulus intensity in panel a with the trunk in the flexed position. (c) Average data for one subject for multiple and single stimuli delivered to the left phrenic nerve at the high-intensity level with the trunk held in a neutral position. Stimulation in this position produced a pressure and torque of lesser magnitude than in the flexed position.

It is evident from the anatomy that the spine is built to resist larger load and torque caudally (e.g. larger vertebrae and larger total muscle cross sections caudally). The reason for this is most likely that in almost all physiological loading situations the external load calling for back extensor torque production is a force pushing the upper body forward (applied through the arms or directly to the back). Such a force will generate progressively larger flexion torques and spinal loads caudally. This fits nicely with our model calculated maximal total back extension torques. The model calculated maximal torques about the four most rostral discs plotted as a function of lever arm length to the external load were, for all subjects, situated close to the linear regression line fitted to them. No data point was, for any individual subject, separated from the regression line by more than 1.4% of the maximal L5/S1 torque in the extended position. Torques about the two most caudal discs were, however, clearly beneath the line (figure 3.10 shows group mean values). The specific back extensor muscle tension needed to fit the equilibrium demands as described in figure 3.10 would be 25±6.0 N/cm^2 in the most flexed and 8.1±1.0 N/cm^2 in the most extended MR position. The higher value lay well within the range from *in vitro* measurements of maximal specific muscle tension, as presented in section

1.3.6. One reason why other studies (e.g. Bogduk et al., 1992) have reported substantially higher maximal muscle tensions is most likely methodological differences in determining muscle fascicle cross sectional areas, as discussed in section 1.3.5. The reasonable adherence to simultaneous equilibrium as well as the realistic maximal muscle tensions obtained when modelling maximal efforts strengthen our confidence in the current biomechanical model.

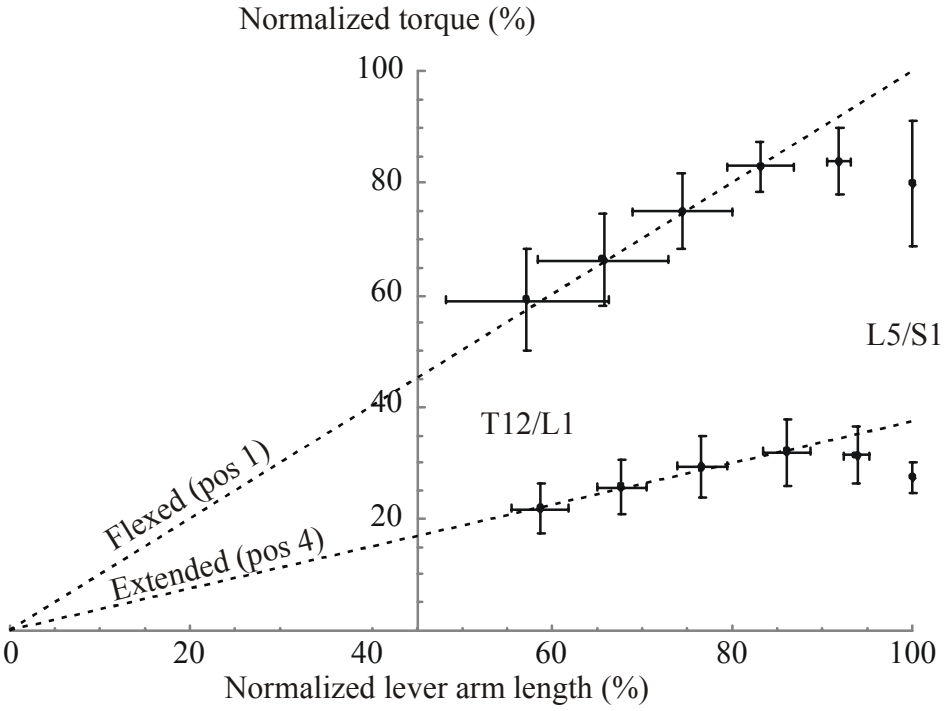

Figure 3.10. Model calculated torques created by back extensor muscles and IAP about disc centres from T12/L1 to L5/S1, normalized to the maximum L5/S1 torque in the maximally flexed MR position (interpolated from torque measurements) plotted against the lever arm length to the external force normalized to its length about the L5/S1 disc centre. The subjects' muscle tensions were set to make a least square fit of the four leftmost data points (T12/L1 to L3/L4) to the external torque. Group mean values (± 1SD) for the most flexed and the most extended position in the MR-camera are presented. Differences between lever arm lengths to the external force (assumed to act perpendicular to the mid-thoracic spine), between the different disc centres were measured on the MR-images. The subjects' absolute values of the lever arm lengths were set to make the linear regression lines for the four leftmost data points pass through the origin. The dotted lines represent the torque created by the external force.

We could look upon the equilibrium mismatch about the two most caudal discs as earlier investigators have (Stokes and Gardner-Morse, 1995) and assume that the model is correct, which would lead to the conclusion that many fascicles of the back extensor muscles could not be fully activated during maximal back extensions and that static equilibrium would involve a complex motor control task with independent regulation of the force in individual muscle fascicles. As stated in section 2.4.2 it is more likely that the back extensor muscles to a large extent are close to maximally activated during maximal static back extension and that the equilibrium is maintained passively by changes of spinal posture leading to changes in muscle forces due to changes in muscle length. The mismatch between model predictions of the torques created by the external load and the muscle and IAP generated maximal torques at the two most caudal levels, is most likely due to discrepancies between model and reality. Some possible causes might be underestimation of fascicle cross-sectional areas of back extensor muscle

fascicles with their caudal origin on L4 and L5 or torque contribution from passive forces in discs, ligaments or facet joints. Although further investigations are needed to clarify this, there are some indications that the iliolumbar ligament might be loaded during maximal back extensions (Leong et al., 1987). Any such extra forces acting on the two most caudal vertebrae would give rise to additional loads on the L4/L5 and L5/S1 discs, i.e. the calculated forces on these discs are most likely underestimated here.

3.5 CONCLUDING REMARKS

This thesis has contributed to the development of a realistic lumbar back extensor model by expanding the detailed information of back extensor muscle anatomy, by clarifying the possible effects of intra-abdominal pressure on lumbar extension torque generation and spinal unloading, by demonstrating how changes in lumbar flexion-extension can alter the mechanics of lumbar back extension and by discussing other issues like measurement of physiological cross-sectional areas and the motor control of back extensor muscles. The developed model was tested by comparisons with relevant physiological measurements and showed, in most cases, a reasonable agreement. The results will have consequences for our understanding of back extension in the context of injury mechanisms, rehabilitation as well as sports and workplace performance.

The model developed here will certainly be modified and developed further by future research. As I see it, the most important studies for the near future would be a detailed investigation of the back extensor muscle activity during maximal exertions, measurements of the individual back extensor muscles sarcomere lengths in a given trunk posture as well as development of methods for reliable, *in vivo*, estimations or measurements of forces in passive tissues, such as ligaments.

4 ACKNOWLEDGEMENTS

I express my warmest thanks to

Alf Thorstensson, for friendly and stimulating supervision and support, for trusting me with freedom although years have passed and for being of invaluable help in the writing process.

Per Tveit for contributing the idea and the data collection for study I as well as for sharing friendship and good times in Stockholm and Oslo.

Qiang-Min Huang for being such a character, for his skilful dissections in study III, for dimplings, chicken feet and friendship.

Paul Hodges for contributing the lion part of study IV, for his enthusiastic approach to biomechanics and for his generous ways.

Andrew Cresswell for contributing to study IV, for lots of help on computer issues and for his ambitious work on behalf of the lab.

To present and former members of the Biomechanics and Motor Control Laboratory for making life at work so much more fun and for their friendship and support; Eva Andersson, Carl Askling, Britt Arvidsson, Anna Bjerkefors, Trish Blake, Anatoli Grigorenko, Marketta Henriksson, Wolfgang Löscher, Johnny Nilsson, Lee Nolan, Maria Nordlund, Kristjan Oddsson, Lars Oddsson, Thomas Persson, Gavin Pinniger, Hans Rosdahl, Jan Seger, Ari Sirin, Virgil Stokes.

Alexander Ovendal for his friendship at the lab and for always helping out with everything, including being the default subject.

Jöran Thell and Gabriel Berg for being good friends and durable subjects (not backing out even after IAP catheter induced vomiting).

All other subjects for their contribution of time and effort.

Mia Lindskog, Rita Almeida and Anders Ledberg for their friendship and for creating fun and exciting scientific projects pleasantly far away from lumbar back extensions. We still have to break the neural code one day.

All other doctoral students of neuroscience whom I have spent time with in rewarding discussions, ski-slopes and dance floors.

Bo Nordell and all the others at the MR centre for friendly and professional assistance.

The Visible Human Project from the US National Library of Medicine for conceiving, generating and sharing their image data.

The anatomy department at the Karolinska Institute for giving access to cadavers.

George Goertz, Eddy Karlsson, Styrbjörn Bergelt for their pleasant personalities and their professional craftsmanship.

Everyone else at “the other side” (Lidingövägen 2.) for Christmas parties, pleasant lunch company and generally for contributing to a good atmosphere.

Idrottshögskolan, the Swedish Work Environmental Fund, the Swedish Medical Research Council and the Centre for Sport Research for their financial support.

Anna Nordlander, Ninni Eglén, Viveca Thors, Anna Ruhr and Polina Kontogianni for sharing love and friendship. You are the evolutionary reason why men bother writing theses.

Louise Arve, Ramon Malawe, Lotta Fredholm and Zebo Hillborg for being always trusted friends to share wine (beer for Ramon) and confidences with.

All friends from IK Stadion (no one mentioned and no one forgotten), Raymond Young and all other friends from the Karate as well as Bela Rerrich and all other friends from Djurgårdens fäktklubb for the friendship, excitement, pleasure and mental recharging experienced in the halls of sport.

My parents as well as my brothers with their families for their unconditional support and love.

My grandmother for her companionship and support through the years.

All other relatives who, in one way or another, have encouraged and inspired me.

Everybody else who in any way contributed to this work. There are so many small contributions that I cannot list them all, and maybe also some larger ones that I might have forgotten (my apologies in that case).

5 REFERENCES

Ackerman, M.J., Spitzer, V.M., Scherzinger, A.L., and Whitlock, D.G., 1995. The Visible Human data set: an image resource for anatomical visualization. Medinfo 8 Pt 2, 1195-8.

Aleksandrov, A.D., Kolmogorov, A.N., and Lavrent'ev, M.A., 1999. Mathematics, its content, methods and meaning. Dover publications, New York.
Originally published: 1956

Andersson, E.A., Oddsson, L.I., Grundstrom, H., Nilsson, J., and Thorstensson, A., 1996. EMG activities of the quadratus lumborum and erector spinae muscles during flexion-relaxation and other motor tasks. Clin Biomech (Bristol, Avon) 11, 392-400 .

Aristotle, 1984. Complete work of Aristotle, Volume 1, The revised Oxford translation. Princeton university press, Princeton.
Originally published: 4th century BC

Aspden, R.M., 1989. The spine as an arch. A new mathematical model. Spine 14, 266-74.

Bartelink, D.L., 1957. The role of abdominal pressure in relieving the pressure on the lumbar intervertebral discs. Journal of Bone and Joint Surgery. British Volume 39, 718-725.

Benedikt, M., 1910.Biomechanische Grundfragen, offenes Sendschreiben an Herrn Hofrat Ernst Ludwig. Leipzig, Engelmann, W.

Bogduk, N., 1980. A reappraisal of the anatomy of the human lumbar erector spinae. Journal of Anatomy 131, 525-40.

Bogduk, N., Macintosh, J.E., and Pearcy, M.J., 1992. A universal model of the lumbar back muscles in the upright position. Spine 17, 897-913.

Bottinelli, R., Canepari, M., Pellegrino, M.A., and Reggiani, C., 1996. Force-velocity properties of human skeletal muscle fibres: myosin heavy chain isoform and temperature dependence. Journal of Physiology 495 (Pt 2), 573-86.

Bottinelli, R., Pellegrino, M.A., Canepari, M., Rossi, R., and Reggiani, C., 1999. Specific contributions of various muscle fibre types to human muscle performance: an in vitro study. Journal of Electromyography and Kinesiology 9, 87-95.

Boyer, C.B., 1949. The history of the calculus and its conceptual development. Dover Publications, New York.

Bustami, F.M., 1986. A new description of the lumbar erector spinae muscle in man. Journal of Anatomy 144, 81-91.

Chaffin, D.B., 1969. A computerized biomechanical model, development and use in studying gross body actions. Journal of Biomechanics 2, 429-41.

Chaffin, D.B., Redfern, M.S., Erig, M., and Goldstein, S.A., 1990. Lumbar muscle size and locations from CT scans of 96 women of age 40 to 63 years. Clinical Biomechanics 5, 9-16.

Cresswell, A.G., Grundstrom, H., and Thorstensson, A., 1992. Observations on intra-abdominal pressure and patterns of abdominal intra-muscular activity in man. Acta Physiologica Scandinavica 144, 409-18.

Davis, P.R., 1956. Variations of the intra-abdominal pressure during weight lifting in various positions. Journal of Anatomy 90, 601.

De Ruiter, C.J. and De Haan, A., 2000. Temperature effect on the force/velocity relationship of the fresh and fatigued human adductor pollicis muscle. Pflugers Archiv. European Journal of Physiology 440, 163-70.

Dugas, R., 1988. A history of mechanics. Dover publications, New York.

Dumas, G.A., Poulin, M.J., Roy, B., Gagnon, M., and Jovanovic, M., 1991. Orientation and moment arms of some trunk muscles. Spine 16, 293-303.

Edgerton, V.R., Roy, R.R., and Apor, P. 1986 Specific tension of human elbow flexor muscles. In Biochemistry of exercise VI. Human Kinetics, Champaign, IL, Pp. 487-500.

Eldred, E., Ounjian, M., Roy, R.R., and Edgerton, V.R., 1993. Tapering of the intrafascicular endings of muscle fibers and its implications to relay of force. Anatomical Record 236, 390-8.

Galilei, G., 1954. Dialogues Concerning Two New Sciences. Dover Publications, New York. Originally published: 1638

Gandevia, S.C. and McKenzie, D.K., 1986. Human diaphragmatic EMG: changes with lung volume and posture during supramaximal phrenic stimulation. Journal of Applied Physiology 60, 1420-8.

Gans, C., 1982. Fiber architecture and muscle function. Exercise and Sport Sciences Reviews 10, 160-207.

Gibbs, J.W. and Wilson, E.B., 1960. Vector analysis. Dover publications, New York. Originally published: 1901

Gordon, A.M., Huxley, A.F., and Julian, F.J. , 1966. The variation in isometric tension with sarcomere length in vertebrate muscle fibres. Journal of Physiology 184, 170-92.

Grillner, S., Nilsson, J., and Thorstensson, A., 1978. Intra-abdominal pressure changes during natural movements in man. Acta Physiologica Scandinavica 103, 275-83.

Jonsson, B., 1970. The functions of individual muscles in the lumbar part of the spinae muscle. Electromyography 10, 5-21.

Kawakami, Y., Nakazawa, K., Fujimoto, T., Nozaki, D., Miyashita, M., and Fukunaga, T., 1994. Specific tension of elbow flexor and extensor muscles based on magnetic resonance imaging. Eur J Appl Physiol Occup Physiol 68, 139-47.

Keith, A., 1923. Mans posture: Its evolution and disorders. Lecture IV. The adaptations of the abdomen and its viscera to the orthograde posture. British Medical Journal 1, 587-590.

Kumar, S., 1988. Moment arms of spinal musculature determined from CT-scans. Clinical Biomechanics 3, 137-144.

Leong, J.C., Luk, K.D., Chow, D.H., and Woo, C.W., 1987. The biomechanical functions of the iliolumbar ligament in maintaining stability of the lumbosacral junction. Spine 12, 669-74.

Lindberg, D.A. and Humphreys, B.L., 1995. Computers in medicine. JAMA 273, 1667-8.

Macintosh, J.E. and Bogduk, N., 1986. The morphology of the human lumbar multifidus. Clinical Biomechanics 1, 196-204.

Macintosh, J.E. and Bogduk, N., 1987. 1987 Volvo award in basic science. The morphology of the lumbar erector spinae. Spine 12, 658-68.

Macintosh, J.E. and Bogduk, N., 1991. The attachments of the lumbar erector spinae. Spine 16, 783-92.

Macintosh, J.E., Bogduk, N., and Pearcy, M.J., 1993. The effects of flexion on the geometry and actions of the lumbar erector spinae. Spine 18, 884-93.

MacLean, I.C. and Mattioni, T.A., 1981. Phrenic nerve conduction studies: a new technique and its application in quadriplegic patients. Archives of Physical Medicine and Rehabilitation 62, 70-3.

McGill, S.M., 1988. Estimation of force and extensor moment contributions of the disc and ligaments at L4-L5. Spine 13, 1395-402.

McGill, S.M. and Norman, R.W., 1986. Partitioning of the L4-L5 dynamic moment into disc, ligamentous, and muscular components during lifting. Spine 11, 666-78.

McGill, S.M. and Norman, R.W., 1987a. Effects of an anatomically detailed erector spinae model on L4/L5 disc compression and shear. Journal of Biomechanics 20, 591-600.

McGill, S.M. and Norman, R.W., 1987b. Reassessment of the role of intra-abdominal pressure in spinal compression. Ergonomics 30, 1565-88.

McGill, S.M., Patt, N., and Norman, R.W., 1988. Measurement of the trunk musculature of active males using CT scan radiography: implications for force and moment generating capacity about the L4/L5 joint. Journal of Biomechanics 21, 329-41.

McNally, D.S. and Adams, M.A., 1992. Internal intervertebral disc mechanics as revealed by stress profilometry. Spine 17, 66-73.

Morris, S.M., Lucas, D.M., and Bresler, B., 1961. Role of the trunk in stability of the spine. Journal of Bone and Joint Surgery 43, 327-351.

Nemeth, G. and Ohlsen, H., 1986. Moment arm lengths of trunk muscles to the lumbosacral joint obtained in vivo with computed tomography. Spine 11, 158-60.

Newton, I., 1999. The Principia, Mathematical principles of natural philosophy. University of California press, Berkely.
Originally published: 1687

Nussbaum, M.A., Chaffin, D.B., and Rechtien, C.J., 1995. Muscle lines-of-action affect predicted forces in optimization-based spine muscle modeling. Journal of Biomechanics 28, 401-9.

Reid, J.G., Costigan, P.A., and Comrie, W., 1987. Prediction of trunk muscle areas and moment arms by use of anthropometric measures. Spine 12, 273-5.

Spitzer, V., Ackerman, M.J., Scherzinger, A.L., and Whitlock, D., 1996. The visible human male: a technical report. Journal of the American Medical Informatics Association 3, 118-30.

Stienen, G.J., Kiers, J.L., Bottinelli, R., and Reggiani, C., 1996. Myofibrillar ATPase activity in skinned human skeletal muscle fibres: fibre type and temperature dependence. Journal of Physiology 493 (Pt 2), 299-307.

Stokes, I.A. and Gardner-Morse, M., 1995. Lumbar spine maximum efforts and muscle recruitment patterns predicted by a model with multijoint muscles and joints with stiffness. Journal of Biomechanics 28, 173-86.

Thomson, K.D., 1988. On the bending moment capability of the pressurized abdominal cavity during human lifting activity. Ergonomics 31, 817-28.

Thorstensson, A. and Nilsson, J., 1982. Trunk muscle strength during constant velocity movements. Scandinavian Journal of Rehabilitation Medicine 14, 61-8.

Thorstensson, A. and Oddsson, L., 1982. Muscle force per unit cross-sectional area of the trunk extensor muscles in men and women. Acta Physiologica Scandinavica 41A.

Trotter, J.A., 1993. Functional morphology of force transmission in skeletal muscle. A brief review. Acta Anatomica 146, 205-22.

Williams, P.L. et al. (Eds.), 1995. Gray's Anatomy 38th edition. Churchill Livingstone, Edinburgh.

Winkler, G., 1937. La structure du muscle spinalis dorsi chez l'homme. Archives d'Anatomie, d'Histologie et d'Embryologie 23, 183-206.